



Effects of Wildfires on Lakes

Study report: Regional and global impact of wildfires on lakes

Reference: CCI-LAKES-0080-RP

Issue: 1.1

Date: 31/01/2023

Version history:			
Issue:	Date:	Reason for change:	Author
1.0	31 January 2023	Initial Version	C. Giardino M. Pinardi R. Caroni D. Stroppiana M. Bresciani G. Tellina L. Parigi
1.1	16 February 2023	Internal Review	S. Simis J.F. Crétaux

People involved in this issue:			Signature
Authors:	Claudia Giardino Monica Pinardi Rossana Caroni Daniela Stroppiana Mariano Bresciani Giulio Tellina Lorenzo Parigi	CNR	
Approved by:	Alice Andral po Bruno Coulon	CLS	
Reviewed by:	Stefan Simis J.F. Crétaux	PML	
Authorized by:	Clément Albergel	ESA	

Distribution:		
Company	Names	Contact Details
ESA	C. Albergel	Clement.Albergel@esa.int
CLS	B. Coulon B. Calmettes A. Mangilli P. Thibaut	bcoulon@groupcls.com bcalmettes@groupcls.com amangilli@groupcls.com pthibaut@groupcls.com
Eola	E. Zakharova	zavocado@gmail.com
H2OG	C. Duguay	claude.duguay@h2ogeomatics.com
LEGOS	J.F. Crétaux A. Kouraev	jean-francois.cretaux@legos.obs-mip.fr kouraev@legos.obs-mip.fr
PML	S. Simis	stsi@pml.ac.uk
CNR	C. Giardino	giardino.c@irea.cnr.it

List of Contents

1. Background and objectives	6
2. Chlorophyll-a data preparation and lake trophic status classification	8
2.1 Methods	8
2.2 Results	8
3. Definition of lake catchments and fire data preparation	9
4. Source - Pathway - Receptor (SPR) approach	11
4.1 Selection of lakes	11
4.2 Methods	11
4.3 Results	11
5. Assessing the impact of wildfires on pristine lakes globally	18
5.1 Impact of burned area on annual Chl-a average values	18
5.2 Relationship between Chl-a daily anomalies and burned areas	19
6. Investigation of WFD priority substances data for assessing wildfire impacts on lakes	27
6.1 Background	27
6.2 Methods	28
6.3 Results	28
7. Conclusions	33
8. References	35
9. Annex 1	38
10. Annex 2	39

LIST OF TABLES AND FIGURES

Table 2-1. Lake trophic status classification based on mean chlorophyll-a concentration.....	8
Table 4-1. Contingency matrix of 2024 lakes selected via two clustering procedures: land type cover burned in 2011 (rows representing clusters 1-6 and total area burned from 2011-2020 (columns representing clusters 1,2,6,10,35 and 80). Potential geographical and land cover combinations with burn temporal pattern (frequency/intensity) clusters are highlighted in bold (n = 314).	11
Table 4-2. Lake geomorphological and trophic status characteristics, major fire events and responses in water chlorophyll-a (Chl-a) and/or Turbidity (NTU) concentrations of the lake subset during 2017-2020.	13
Table 5-1. Lake’s identification, characteristics (trophic state, altitude, area, maximum depth), year of the fire event to be investigated for fire effects on water quality and land cover of the burned area pixels are reported.....	20
Figure 2-1. Pie chart of the trophic status classification of lakes included in the Lakes_cci dataset (period 2016-2020) and global map of lakes classified as ultra- and oligotrophic.	8
Figure 3-1 Flowchart for the definition of lake catchments. Numbers in each box show the number of polygons contained in each layer.	9
Figure 3-2. The number of lake catchments in each continental area as a function of the maximum number of iterations necessary to build the catchment (x-axis).....	10
Figure 3-3. Example of the output lake catchments for peri-alpine lakes (a) and Northern Europe (b). Each colour represents a relation to a specific lake.....	10

Figure 4-1. Lakes from contingency matrix further selected to have a SPI 95th percentile above 1.5 and a catchment area / lake area above 30 (i.e., upper right quarter of graph). The number of clusters refers to Table 4-1. 12

Figure 4-2. Localization of the 154 lakes identified in the upper right quarter of graph of Figure 4-2 from the contingency matrix. The number of clusters refers to Table 4-1. 13

Figure 4-3. Graphs of burned area, standardised precipitation index (SPI), lake surface water temperature (LSWT), ice cover (sum_ROIs_ice), chlorophyll-a (Chl-a) and Turbidity (NTU) for the 9 lakes selected with seasonal ice cover. 16

Figure 4-4. Graphs of burned area, standardised precipitation index (SPI), lake surface water temperature (LSWT), ice cover (sum_ROIs_ice), chlorophyll-a (Chl-a) and Turbidity (NTU) for the 9 lakes selected with seasonal ice cover. 17

Figure 5-1. Scheme of the statistical tests carried out between fire and no fire/control years. 18

Figure 5-2. Boxplots of control (C, green), Fire (F, red) and post-fire (A1, light blue) weekly average Chl-a concentration (y-axis) for the pristine lakes under analysis (x-axis). In some cases, post-fire A1 year is not available, according to the method applied. 19

Figure 5-3. Plot of positive and negative Chl-a anomaly (Delta Chl-a) with Chl-a reference (Chl-a clim) (a, c, e), and plot of Chl-a anomaly ratio (Delta-ratio Chl-a) with burned area (b, d, f) for Lake Flathead (US; Lake_ID 375), Lake Bear (US; Lake_ID 677), and Lake Terewah/Narran (Australia; Lake_ID 1726), respectively. 21

Figure 5-4. Plot of positive and negative Chl-a anomaly (Delta Chl-a) with Chl-a reference (Chl-a clim) (a), and plot of Chl-a anomaly ratio (Delta-ratio Chl-a) with burned area (b) for Lake Pasfield (Canada; Lake_ID 782). 22

Figure 5-5. Plot of positive and negative Chl-a anomaly (Delta Chl-a) with Chl-a reference (Chl-a clim) (a, c), and plot of Chl-a anomaly ratio (Delta-ratio Chl-a) with burned area (b, d) for Lake Pyramid (US; Lake_ID 411) and Lake Puelo (Argentina; Lake_ID 300010602), respectively. 22

Figure 5-6. Maps of Lake Flathead (upper panel) and Lake Terewah/Narran (lower panel) with their catchments and burned area (BA) distribution and occurrence (DOY). The graphs report Chlorophyll-a (Chl-a, green) and Turbidity (red) concentrations, total precipitation (tp, blue) and BA histograms (gray). 23

Figure 5-7. Chlorophyll-a maps of Lake Flathead (ID_375; US) in the summer 2003 and 2004, that is immediately after and one year after the fire events. Fires occurred in March and September 2003. 24

Figure 5-8. Turbidity and chlorophyll-a maps of Lake Terewah/Narran (ID_1726; AUS) in the pre- and post-fire period of 2003 and a year after the fire in 2004, respectively. Fires occurred from March to October 2003. 24

Figure 5-9. Maps of Lake Pyramid (ID_411) (upper panel) and Lake Puelo (ID_300010602) (lower panel) with their catchments and burned area (BA) distribution and occurrence (DOY). The graphs report Chlorophyll-a (Chl-a, green) concentrations, total precipitation (tp, blue) and BA histograms (gray). 25

Figure 5-10. In the upper panel chlorophyll-a maps of Lake Pyramid (ID_411; US) in the season following fire events of 2017. Fires occurred between July and September 2017. In the lower panel Chl-a maps of Lake Puelo (ID_300010602; AR) in the post-fire period of 2016. Fires occurred in March and April 2015. 26

Figure 6-1. Scheme of the approach used to merge the Lakes_cci dataset with European reporting WISE dataset. The number reported in brackets refers to the number of lake stations obtained as output. 29

Figure 6-2. Lake Corrib (IE) location and fire site active during May 2016 (DOY of burned pixel detection). 30

Figure 6-3. Fluoranthene and Benzo(a)pyrene concentration in 2016 in Lake Corrib. 30

Figure 6-4. Wind diagram for the period April-May 2016 around Lake Corrib. 30

Figure 6-5. Fluoranthene and Naphthalene concentration in 2018/2019 in Lake Batak. 31

Figure 6-6. Lake Batak (BG) location and fire site active during 2018 (DOY of burned pixel detection). 31

Figure 6-7. Wind diagrams for the summer and autumn period of fires in 2018 around Lake Batak. 32

1. Background and objectives

Since decades it is evident that climate change is generating complex responses in aquatic ecosystems that vary according to their geographic distribution, magnitude, and timing across the global landscape (e.g., Williamson et al., 2009). Climate change, in particular global warming and increasing aridity, is leading to an increase of fire frequency and severity (Brown et al., 2021). Fire is a prevalent feature of many landscapes. It has numerous and complex effects on geological, hydrological, ecological, and economic systems. Landscapes exposed to fire often include stream, river and lake catchments leading to cascade effects up to the loss of ecosystem services they provide (Smith et al., 2011). In fact, lakes are naturally downstream recipients and integrators of transport from land to water and of processes that occur in their watersheds (Williamson et al., 2008).

Two main pathways for the relationship between fires and water characteristics can be identified: i) atmospheric transport of compounds from fire emissions and deposition over lake waters; ii) increased soil erosion and changes in runoff due to vegetation removal and sediment transport through the river network to lakes. Wildfire emissions of pollutants through smoke plumes are transported into the atmosphere and, in some cases, far from the originating fire event location (Wang et al., 2022). One of the impacts of wildfires is the release of persistent organic pollutants, including polycyclic aromatic hydrocarbons (PAHs). While PAHs generated during wildfires have been sufficiently studied in the atmosphere (e.g., Wentworth et al., 2018) and in soils (e.g., Vergnoux et al., 2011; Campos et al., 2016), studies of PAHs patterns in surface and ground waters are limited (e.g., Smith et al., 2011; Mansilha et al., 2014; Gorshkov et al., 2021). For the second pathway, the fire disturbance on vegetation cover, create an ash layer rich in potential contaminants, and increase contaminant mobilisation by enhancing runoff and erosion. This may lead to the contamination of surface and groundwater resources with suspended sediments, metals, organic compounds and nutrients. These contaminants can also accumulate in riverbanks, flood plains or at the bottom of rivers and lakes, creating problems long after the fires end. The magnitude and duration of hydrological and geomorphological activity following wildfires depends on the complex interplay of factors including site (e.g., catchment size, land cover) and fire characteristics (e.g., severity and extent) as well as post-fire rainfall patterns (Pacheco and Fernandes, 2021). In fact, the magnitude, intensity and frequency of post-fire rainfall and associated flow events are key drivers of erosion and sediment delivery in many burned catchments (Robichaud et al., 2007; Malmon et al., 2007; Cannon et al., 2008; Moody and Martin, 2009).

Changes induced by wildfires can be short lived or last many years. Research on the relationship between wildfires and water quality is largely inter-disciplinary. Long- and short-term impacts of wildfires on the quality of lakes water can be investigated with the use of datasets produced from remote sensing techniques, which provide consistent, global, and objective information and have been increasingly used for monitoring the state of Earth systems (Zhao et al., 2022). Earth Observation (EO) data can support systematic delivery of geospatial products depicting spatio-temporal variation of active fires, burned area and optical-biogeochemical indicators of water quality (e.g., chlorophyll-a and turbidity concentration) worldwide (Warren et al., 2021; Chuvieco et al., 2022; Lizundia-Loiola et al., 2020; Giglio et al., 2009). The specific effects of wildfires on water quality are less commonly reported compared to the effects on terrestrial ecosystems or on the hydrology of burned catchments (Dahm et al., 2015). A deeper understanding of the impact of fires on aquatic ecosystems and water quality is also necessary for the development of adaptation and mitigation strategies.

Investigation of the effects of fire events on lakes are required over short and medium range periods following the event, encompassing different biomes and relying on multitemporal datasets. The overall objective of this study is to use observations from satellites of the fire and lakes Essential Climate Variables (ECVs) and other global data products to examine the impact of wildfires on lakes, in particular on pristine lakes. Pristine lakes are under threat globally due to anthropogenic pressures, and none remain in Europe for several specific lake types (Järvinen et al., 2013). Lakes in remote and remaining wilderness areas globally, previously shielded, now face increasing threats from climate change, including the increased incidence of wildfires. This study takes data from the Fire_cci and Lakes_cci to identify pristine lakes globally likely to be threatened by fire, and subsequently examines key events for potential ecological responses.

This study first introduces chlorophyll-a (Chl-a) data preparation, followed by the classification of the trophic status of all lakes included in the Lakes_cci dataset V2.0.2 (section 2). Then, a section is dedicated to the definition of lake connected catchments to identify terrestrial riverine pathways from burned areas to the recipient lake, and fire data preparation (Fire_cci dataset) (section 3). These first steps feed into all subsequent analyses. A section follows with the explanation of the Source - Pathway - Receptor (SPR) approach to identify lakes that are more prone to wildfire effects (section 4). Section 5 is dedicated to the assessment of the impact of wildfires on pristine lakes at the global level. Finally, we turn the focus of this study to Water Framework Directive (WFD) priority substances (i.e., PAHs) data further detect and investigate impacts of wildfires on lake water (section 6). All these results are followed by a discussion with key conclusions of the work (section 7).

2. Chlorophyll-a data preparation and lake trophic status classification

2.1 Methods

From the Lakes_cci dataset V2.0.2 Chl-a data were extracted for all lakes for the period 2003-2020 (Carrea et al., 2022) and with the R software (R Core Team 2022) the following post-processing of these data was then performed:

- Removal of Chl-a data when Ice Cover data is also present.
- Applying concentration thresholds: $0.00001 < \text{Chl-a} < 300 \text{ mg m}^{-3}$.
- Removal of outliers: values 5x interquartile range.

A classification of lake trophic status was performed on the basis of phytoplankton abundance, that is Chl-a concentration, calculated for the period 2016-2020, according to OECD (1982) (Table 2-1).

Table 2-1. Lake trophic status classification based on mean chlorophyll-a concentration.

Lake category	Chlorophyll-a (mg m^{-3})
Ultra-oligotrophic	< 1
Oligotrophic	<2.5
Mesotrophic	2.5-8
Eutrophic	8-25
Hypertrophic	> 25

2.2 Results

The distribution of the trophic status classification of lakes included in the Lakes_cci dataset is reported in Figure 2-1. A total of 234 lakes were extracted as sum of ultra- (n=107) and oligotrophic (n=127) lakes from the classification of all lakes with the ECV LWLR (Figure 2-1). We assumed that the low trophic status can be a proxy of pristine lakes.

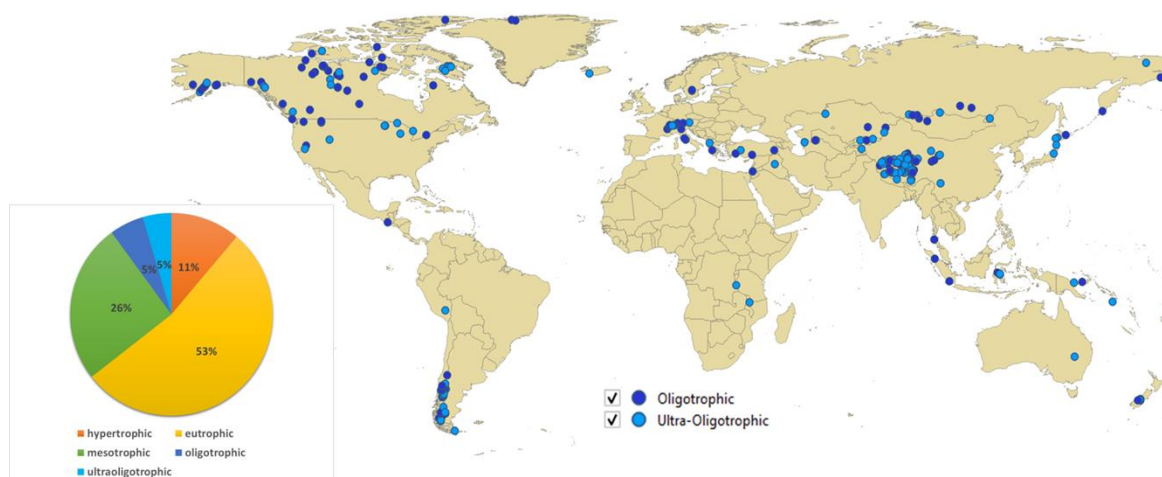


Figure 2-1. Pie chart of the trophic status classification of lakes included in the Lakes_cci dataset (period 2016-2020) and global map of lakes classified as ultra- and oligotrophic.

3. Definition of lake catchments and fire data preparation

A key step in the analysis was the selection of basins connected to each lake. The lake catchment defines the area where fires could influence lake water quality through run-off. Lake catchments were identified from the HydroBASINS product version 1.c (Lehner and Grill, 2013; HydroSHEDS, 2014) which contains polygons defining hierarchically nested sub-basin boundaries at the global scale (from Level 1 to Level 12).

Specifically, we used the following information from the attribute table of the shapefile:

1. "HYBAS_ID": unique basin identifier;
2. "NEXT_DOWN": Hybas_id of the next downstream polygon that can be used for navigation (up- and downstream) within the river network;
3. "LAKE": indicator for lake types: 0 = no Lake; 1 = Lake; 2 = Reservoir; 3 = Lagoon.

The catchment can be identified recursively starting from the lake ID. In this study we defined a global catchment dataset from lakes included in the Lakes_cci (Figure 3-1).

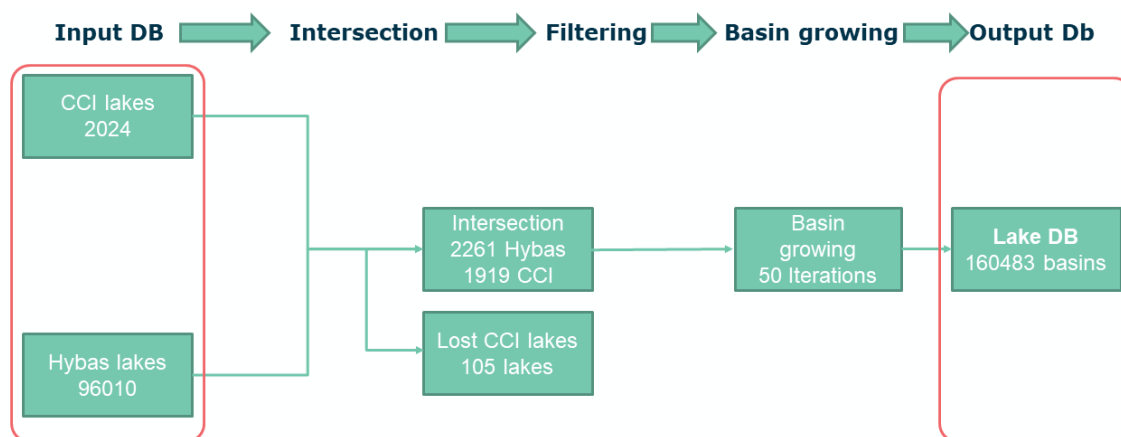


Figure 3-1 Flowchart for the definition of lake catchments. Numbers in each box show the number of polygons contained in each layer.

With the hierarchical information in the HydroBASINS layer it is possible to navigate upstream from the selected lake to all sub-basins hydrologically connected to the lake. We first identified the intersection of lakes contained in Lakes_cci and HydroBASINS. At this stage, 105 lakes included in the CCI dataset were discarded since they were not represented in the HydroBASINS layer (marked as 'Lost' in Figure 3-1). In the basin growing step, a new polygon is connected through the "NEXT_DOWN" attribute under the condition that it is not a new lake based on the "LAKE" attribute. When the script finds a lake it will stop growing connections. The flowchart was implemented in R Language for Statistical Computing (R Core Team, 2022).

The procedure can be repeated until each catchment stops growing. However, we assumed that fires are less relevant in the analysis of the impact on lake water if they occur far from the lake. Hence, the number of iterations should be limited to avoid growing very large catchments. Preliminary analysis allowed us to set a threshold on the maximum number of iterations equal to 50 to identify most of the sub-basins. Figure 3-2 shows that most of the lakes have a basin network that can be recreated using 50 iterations. An example of the output catchments (with 50 iterations) for two regions in Europe is shown in Figure 3-3.

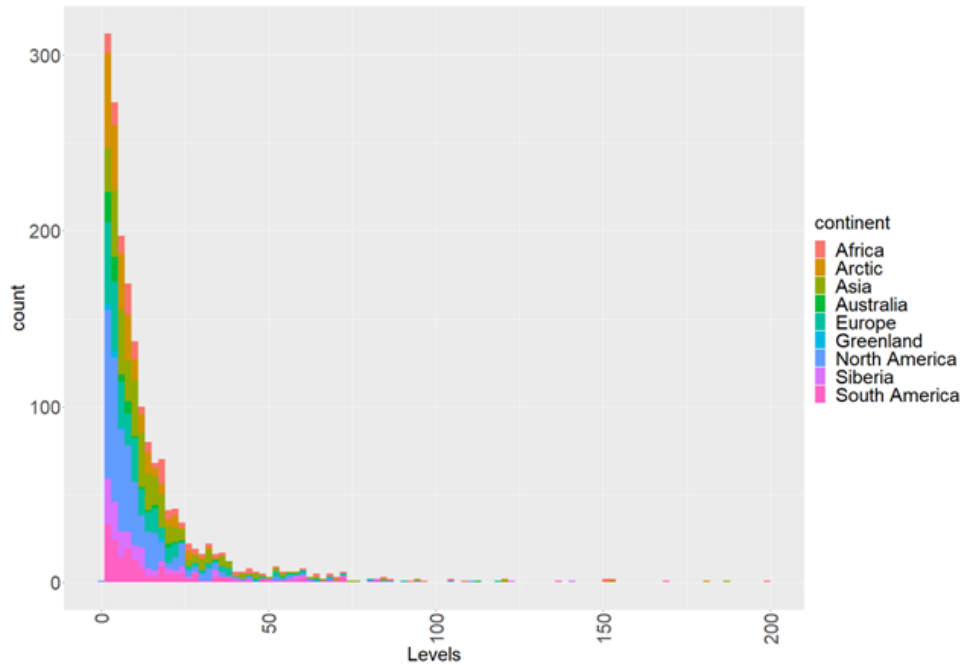


Figure 3-2. The number of lake catchments in each continental area as a function of the maximum number of iterations necessary to build the catchment (x-axis).

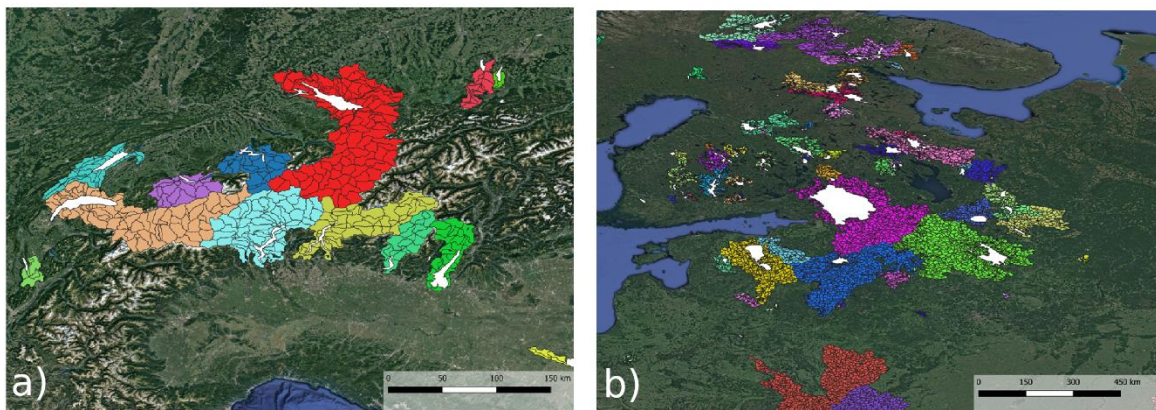


Figure 3-3. Example of the output lake catchments for peri-alpine lakes (a) and Northern Europe (b). Each colour represents a relation to a specific lake.

After the definition of lake catchments the corresponding aggregate burned areas (BA) were extracted. Information on the extent of the area affected by fires for each catchment was extracted from the Fire_cci Burned Area product (FireCCI51) (Lizundia-Loiola et al., 2020) for the period 2001-2020. The FireCCI51 product was downloaded from the Centre for Environmental Data Analysis archive (CEDA, <https://catalogue.ceda.ac.uk/>). Information extracted from the FireCCI51 BA product was, for each burned 250 m pixel: day of the year (DOY) and the land cover according to the Landcover cci project (LC_CCI v2.0.7, ESA, 2017). The FireCCI51 datasets is available as monthly raster GEO tiff files with daily information that was aggregated temporally to weekly and monthly values to enhance peaks/anomalies.

4. Source - Pathway - Receptor (SPR) approach

4.1 Selection of lakes

We explored criteria for selecting lakes most susceptible to fire impacts. The sites were selected according to the Source - Pathway - Receptor (SPR) approach, examining the Lakes_cci dataset (CRDP 2.0.1, Carrea et al., 2022). SPR focuses on identifying the sources, pathways and receptors and their interrelationships, and these are likely key to the understanding of the manifestation of ecosystem alterations caused by wildfires in lakes. In our study, burned areas represent the ‘source’, precipitations (standardised precipitation index-SPI) the ‘pathway’ and lakes (ratio catchment area / lake area) the ‘receptors’.

Starting from a total of 2024 lakes in the Lakes_cci dataset, a series of statistical analyses identified a global subset of lakes likely to be vulnerable to wildfires in their catchments. From the whole dataset of the 2024 lakes and their watersheds, we identified and aggregated types of wildfires, in terms of land cover burned, by means of a hierarchical cluster analysis. The proportion of the hydrological area estimated as burned area over a 20-year period (2001-2020) was also clustered. This resulted in a selection of candidate lakes covering geographical and land cover combinations with different burn temporal patterns (frequency/intensity). The next step of the analysis focussed on the selected lakes, prioritised by their risk from wildfire contamination via riverine input.

4.2 Methods

To identify and aggregate similar types of wildfires, in terms of land cover burned a hierarchical cluster analysis was carried out using Sørensen distance with flexible beta linkage (McCune and Mefford, 2016).

The Standardised Precipitation Index (SPI) was calculated for the period 1980-2019. The SPI calculation for any location is based on the long-term rainfall record for the considered period. This index is a statistical indicator that compares the total (median) precipitation falling at a given location during a given period (12 months for this work) with the distribution of long-term precipitation for the same period (Edwards and McKee, 1997). Negative index values identify moderately to extremely dry conditions, while positive values identify very to moderately wet conditions; values in the range [-1, 1] identify close to normal conditions with respect to the long-term trend.

For the selected lakes, the Lakes_cci products Chl-a and Turbidity were considered as lake water quality parameters that might be affected by wildfires in their catchments. The five largest ROIs per lake were created based on the JRC GSW occurrence layer (Global Surface Water Explorer: global-surface-water.appspot.com). For the period 2017-2020, the weighted mean (by pixel number) per day per lake was calculated, for Chl-a and Turbidity concentrations. Time series for standardised precipitation index (SPI), sum of ice, lake surface water temperature (LSWT) were also produced.

4.3 Results

Cluster analysis of land cover types burned and total area burned provided a total of 314 lakes highlighted for further investigation (Table 4-1). The catchment area/lake area ratio was calculated for these lakes and plotted against the standardised precipitation index (SPI) for the 314 lakes selected from the fire products.

Table 4-1. Contingency matrix of 2024 lakes selected via two clustering procedures: land type cover burned in 2011 (rows representing clusters 1-6 and total area burned from 2011-2020 (columns representing clusters 1,2,6,10,35 and 80). Potential geographical and land cover combinations with burn temporal pattern (frequency/intensity) clusters are highlighted in bold (n = 314).

				Limited regular annual burning	Significant regular annual burning	Limited peak in 2014	Limited peak in 2013	Total
	Cluster	1	2	6	10	35	80	
	1	383	698	128	15	39	18	1281
	2	43	48	14	0	28	12	145
	3	71	19	53	6	1	2	152
Boreal forest (Canada)	4	54	10	13	0	12	6	95
Crops - natural shrubbery (Eurasia)	5	51	0	114	13	1	1	180
Deciduous broad leaves (Africa, India, South America)	6	17	0	93	61	0	0	171
	Total	619	775	415	95	81	39	2024

This allowed us to identify 154 lakes (with a 95th percentile SPI above 1.5, namely dry condition, and a catchment to lake ratio above 30, that is a short residence time) that are likely to be more susceptible to wildfires (Figure 4-1).

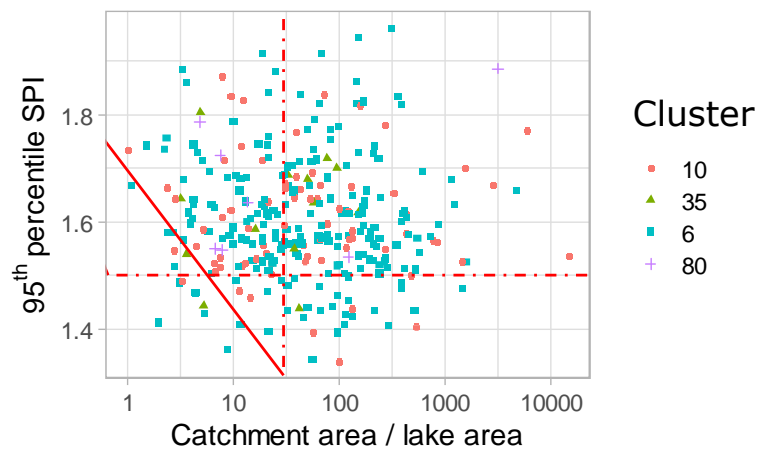


Figure 4-1. Lakes from contingency matrix further selected to have a SPI 95th percentile above 1.5 and a catchment area / lake area above 30 (i.e., upper right quarter of graph). The number of clusters refers to Table 4-1.

Figure 4-2 shows the global distribution of the 154 lakes identified by the contingency matrix.

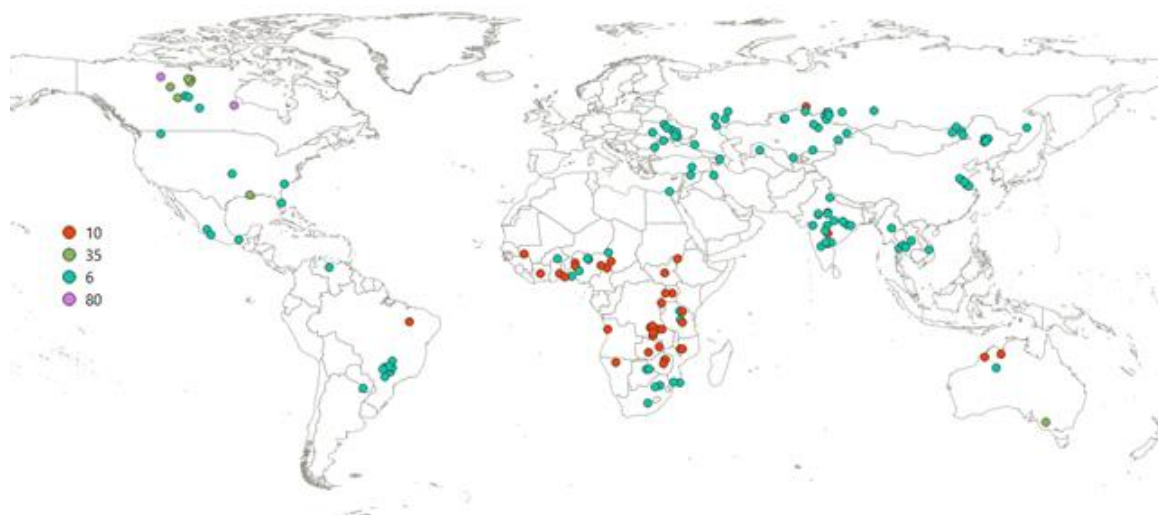


Figure 4-2. Localization of the 154 lakes identified in the upper right quarter of graph of Figure 4-2 from the contingency matrix. The number of clusters refers to Table 4-1.

The next step in our analysis was the use of Lakes_cci products, Chl-a and turbidity, reviewing the selected 154 lakes for data completeness, and to relate the selection to key biomes and fire regimes.

A graphical analysis considering the period 2017-2020 of the Lakes_cci and Fire_cci datasets, compares temporal patterns of Chl-a and Turbidity concentrations with SPI index, ice cover periods and burned areas extension in the catchment of the selected lakes. A subset of lakes, from the 154 candidate lakes, shows lake cases with a correlation in water quality products Chl-a and Turbidity to wildfire occurrence and extension, perhaps due to contamination via precipitation and riverine input. Those lakes have been grouped by absence or presence of ice cover on the lake surface, as ice cover presence may interfere with the detection of water quality products by satellite sensors.

Table 4-2 summarizes lake geomorphological and trophic status characteristics, year of major fire events and responses in water Chl-a and Turbidity concentrations of the lake subset. The average depth of those lakes was less than 20 m, apart from one deeper lake (38.5 m), and lake area was generally >50 km². Lakes were located across a wide range of altitudes and according to the OECD (1982) classification utilized in this report, the trophic state resulted for a majority of lakes to be eutrophic (67%), followed by mesotrophic (28%) and oligotrophic. Major evident responses to fire events, summarized in the table, show lake cases with increase in Chl-a concentration, increases in turbidity, increases in both water quality products, while in a few lakes a decrease in Chl-a was detected.

Graphical analysis for these selected subsets of lakes is reported in Figure 4-3 and Figure 4-4 for the 9 lakes characterized by ice cover and the 9 lakes without ice cover, respectively. The same graphs for the full list of the candidate selected lakes (n=154) can be found in Annex 1.

Table 4-2. Lake geomorphological and trophic status characteristics, major fire events and responses in water chlorophyll-a (Chl-a) and/or Turbidity (NTU) concentrations of the lake subset during 2017-2020.

Lake_ID, Name	Trophic state	Chl-a Mean \pm std (μgL^{-1})	Altitude (m a.s.)	Lake area (km ²)	Average depth (m)	Ice cover	Fire event - Year	Response
Lake 1059, Ukal (India)	Eutrophic	10.2 \pm 5.4	96	370	19.4	no	2018	increase Chl-a and NTU

Study report: Regional assessment on large oligotrophic lakes

Lake 1007, Guarico (Venezuela)	Mesotrophic	3.5±2.8	101	132	9.8	no	2018	increased Chl-a, decreased NTU
Lake 15638, (India)	Eutrophic	12.7±18.6	439	91	15.3	no	2019	increase Chl-a and NTU
Lake 10381, (Paraguay)	Eutrophic	19.5±11.7	56	46	2.2	no	2020	increase Chl-a
Lake 603, Ubol Ratana (Thailand)	Eutrophic	38±29.3	179	313	7.2	no	2019	progressive increase Chl-a
Lake 1612 (Tanzania)	Eutrophic	30.2±27.4	698	443	7.2	no	2019	Chl-a decreased, NTU increased
Lake 1616, Poelela (Mozambique)	Oligotrophic	2.0±1.8	0	88	4.5	no	2018	progressive decrease Chl-a
Lake 15901 (Togo)	Eutrophic	12.0±7.4	0	50	5.3	no	2019	increase Chl-a and NTU
Lake 16311 (Mozambique)	Eutrophic	12.9±8.0	11	54	2.5	no	2018	increase Chl-a and NTU
Lake 502, Balon (Russia)	Eutrophic	50.4±66.7	16	324	12.5	yes	2019	increase Chl-a
Lake 328, Mingechaurskoye (Azerbaijan)	Mesotrophic	5.0±2.2	70	415	38.5	yes	2019	increase Chl-a
Lake 337, Stephens (Canada)	Mesotrophic	4.9±2.1	138	317	8.0	yes	2017	increase Chl-a
Lake 113, Saratov (Russia)	Eutrophic	13.0±14.0	23	1073	12.0	yes	2017	increase NTU and Chl-a
Lake 291, Buir (Mongolia)	Eutrophic	19.6±18.2	577	598	6.3	yes	2017	increase Chl-a and NTU
Lake 601, Krasnodarskoye (Russia)	Eutrophic	8.9±4.9	24	269	11.3	yes	2018	increase NTU
Lake 1609, Uyaly (Kazakhstan)	Mesotrophic	6.8±3.5	348	123	2.0	yes	2019	increase Chl-a, decrease NTU
Lake 13715 (Kazakhstan)	Mesotrophic	6.8±2.3	376	58	4.2	yes	2019	increase NTU
Lake 14041 (China)	Eutrophic	16.8±8.5	146	50	1.0	yes	2019	increase NTU

Study report: Regional assessment on large oligotrophic lakes

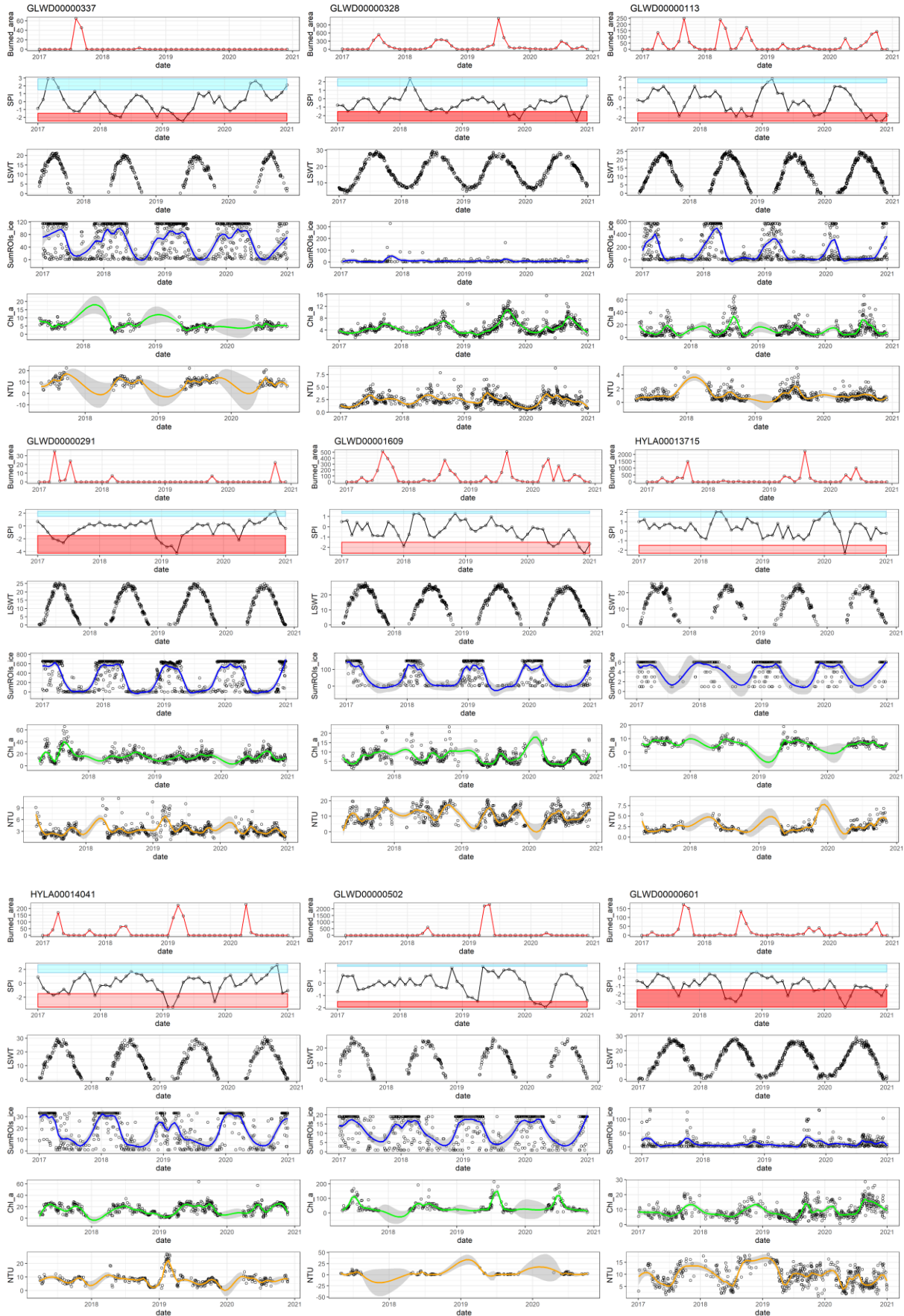
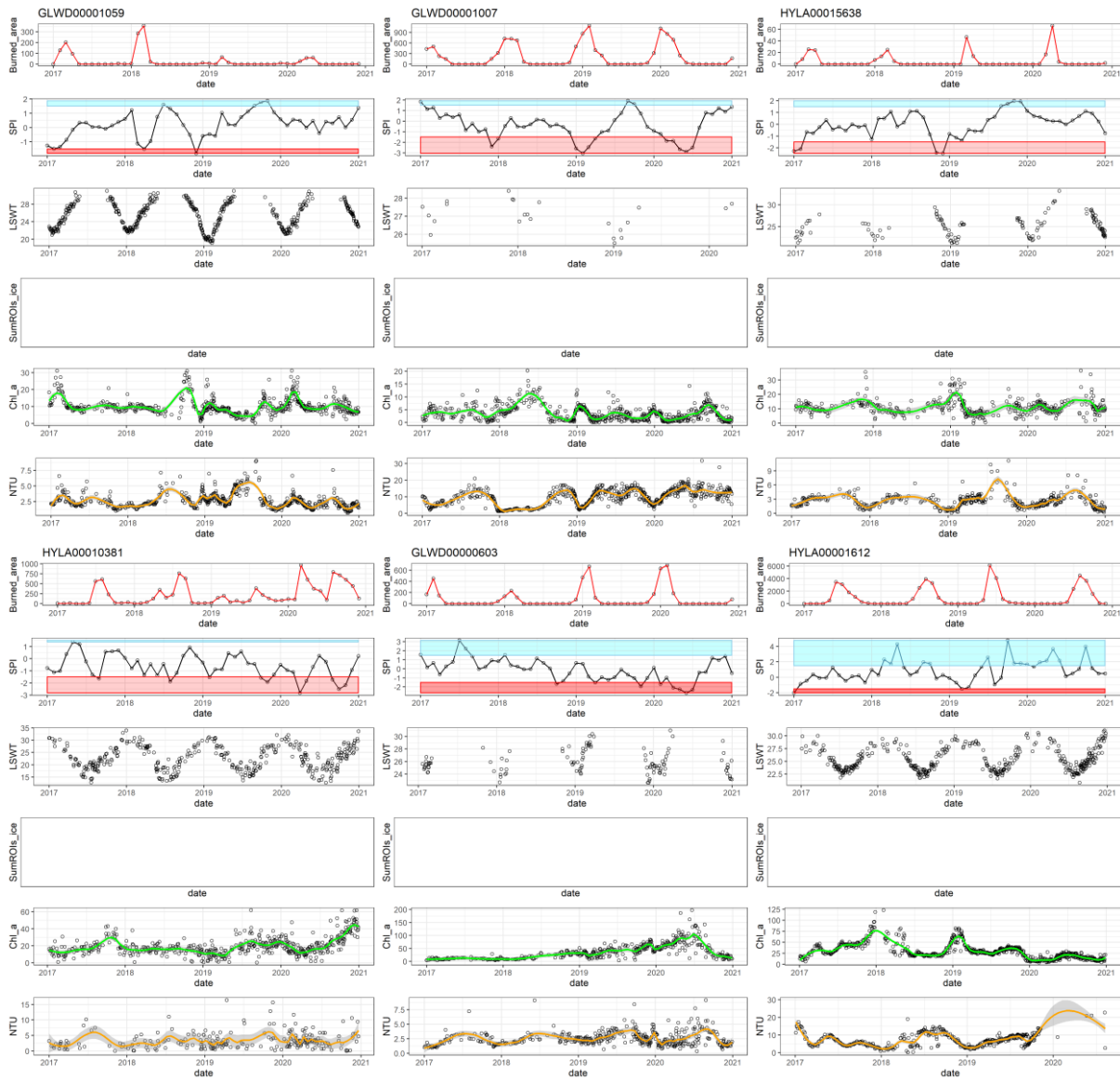


Figure 4-3. Graphs of burned area, standardised precipitation index (SPI), lake surface water temperature (LSWT), ice cover (sum_ROIs_ice), chlorophyll-a (Chl-a) and Turbidity (NTU) for the 9 lakes selected with seasonal ice cover.



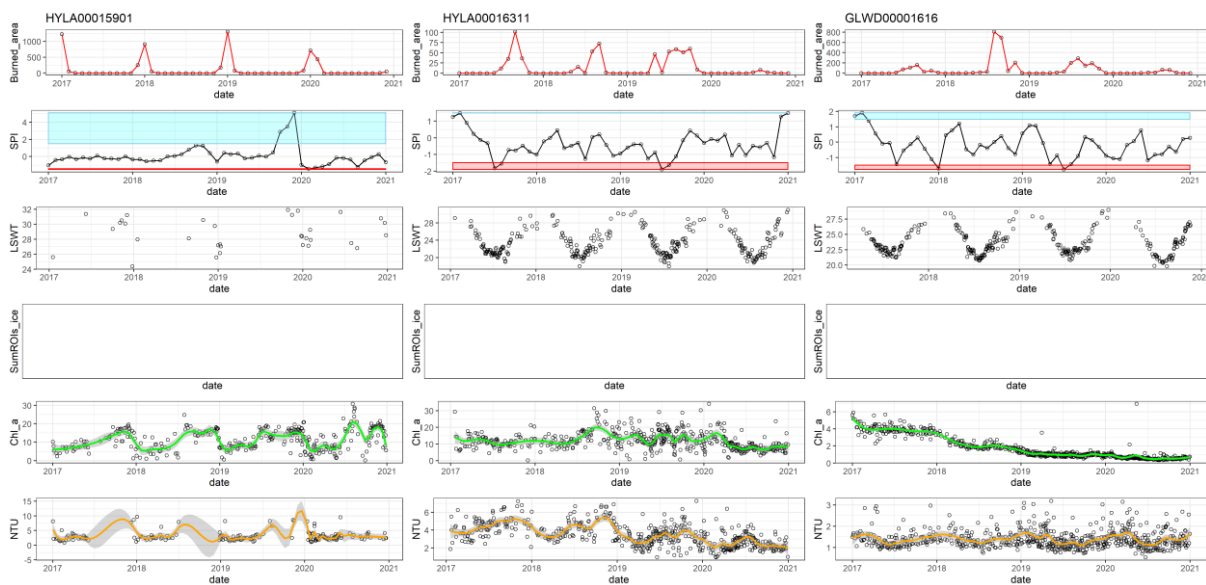


Figure 4-4. Graphs of burned area, standardised precipitation index (SPI), lake surface water temperature (LSWT), ice cover (sum_ROIs_ice), chlorophyll-a (Chl-a) and Turbidity (NTU) for the 9 lakes selected with seasonal ice cover.

5. Assessing the impact of wildfires on pristine lakes globally

5.1 Impact of burned area on annual Chl-a average values

Pristine lakes were identified in section 2 as those lakes with low trophic status (see Figure 2-1). For these lakes, we analysed the correlation between fire occurrence and water quality by assessing whether years with fires showed significantly different levels of Chl-a compared to years with no fire occurrence. The first objective addressed with this analysis was to provide insights on the likely impact of fires at large temporal aggregation scale, i.e., the year. At this level it may be difficult to appreciate the effect of small fires or short-lasting events, but the goal is to test the presence of macroscopic relations and impacts.

Hence, the hypothesis that the fire influences water quality parameters was tested. To assess how fire modifies lake conditions and its long-lasting effects, we compared *fire* and *no fire* periods, where years with low or negligible fire activity are assumed as the baseline for lake water conditions. Wildfires could alter water quality for months and years after the event and no preliminary information on the expected duration is available. Therefore, we assumed as baseline for no fire conditions a period of 1-3 years.

To perform the statistical analysis, the preliminary step was to identify those years with *fire* occurrence and with no fires in preceding year(s) based on total annual BA in the lake catchment. Only those pristine lakes that satisfy this condition were selected for the statistical test (n=37).

We performed a statistical *t-test* between the control year (no fire year before the event, C) and the year with the fire event (F) as well as the years after the event (A1, A2, A3). The first test (F vs. C) aims at highlighting the impact of fires while the second test (C vs. A1, A2, A3) at testing the duration of the impacts (in some cases/ecosystems we could expect that fire impact lasts over the years). In this case, with impact we identify a significant change in lake Chl-a. Figure 5-1 depicts the synthetic scheme of the criteria and tests applied. Notice that if a fire occurs in the years after the event under analysis, search for long lasting effects stops.

Tests were carried out with one to three-years time step. A paired *t-test* was used to compare mean annual Chl-a for the pristine lakes subset that were selected.

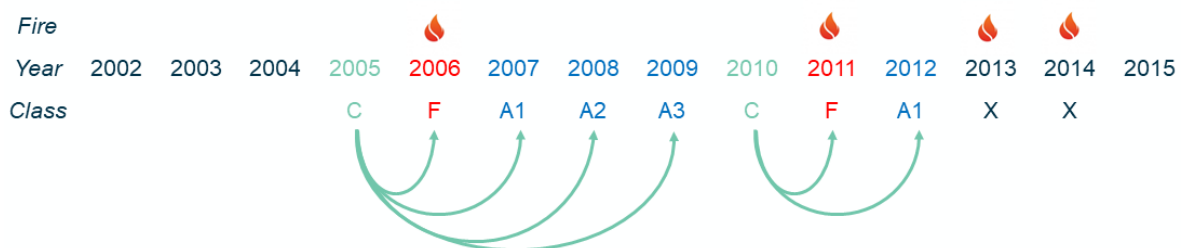


Figure 5-1. Scheme of the statistical tests carried out between fire and no fire/control years.

The results of the paired *t-test* comparing annual average Chl-a of control years and fire event years (F, A1, A2, A3) revealed no significant difference. This result does not mean that there is not a relationship between fire event/burned area and the Chl-a values, but it is not observable at the annual time scale. Furthermore, the lakes under analysis are pristine, but they manifest an important variability in the response to the fire events (

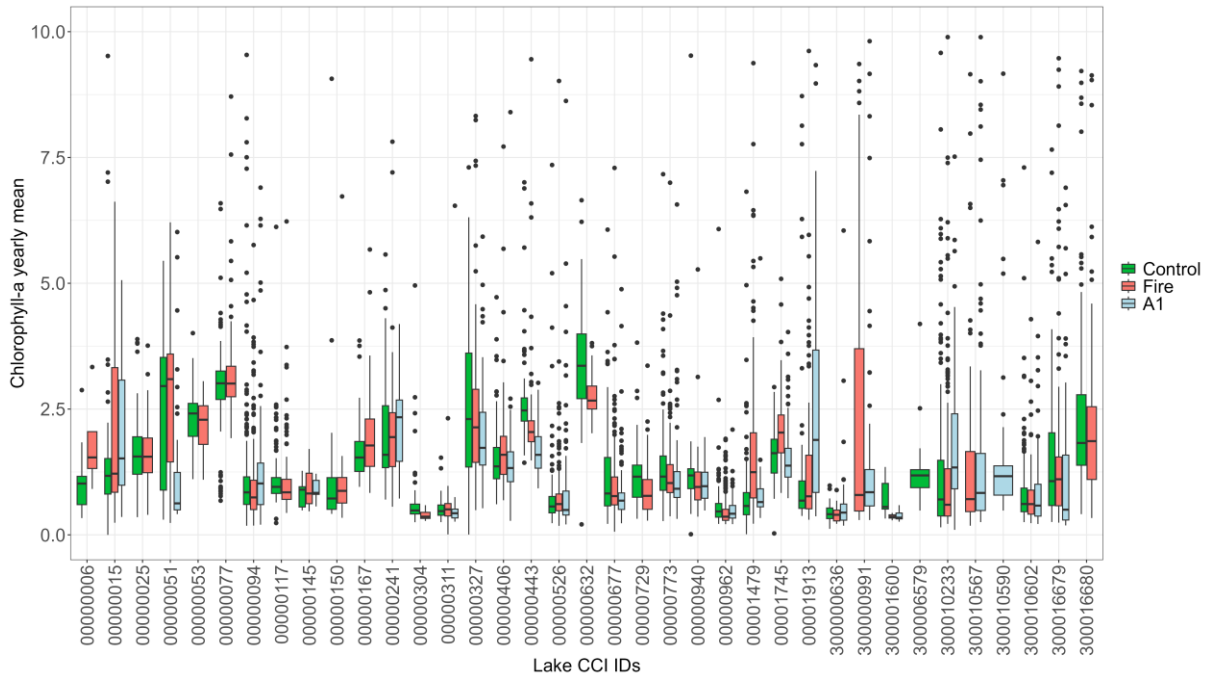


Figure 5-2). Moreover, wildfire events could be variable in terms of severity and extension of burned areas, and there is a need for further investigation.

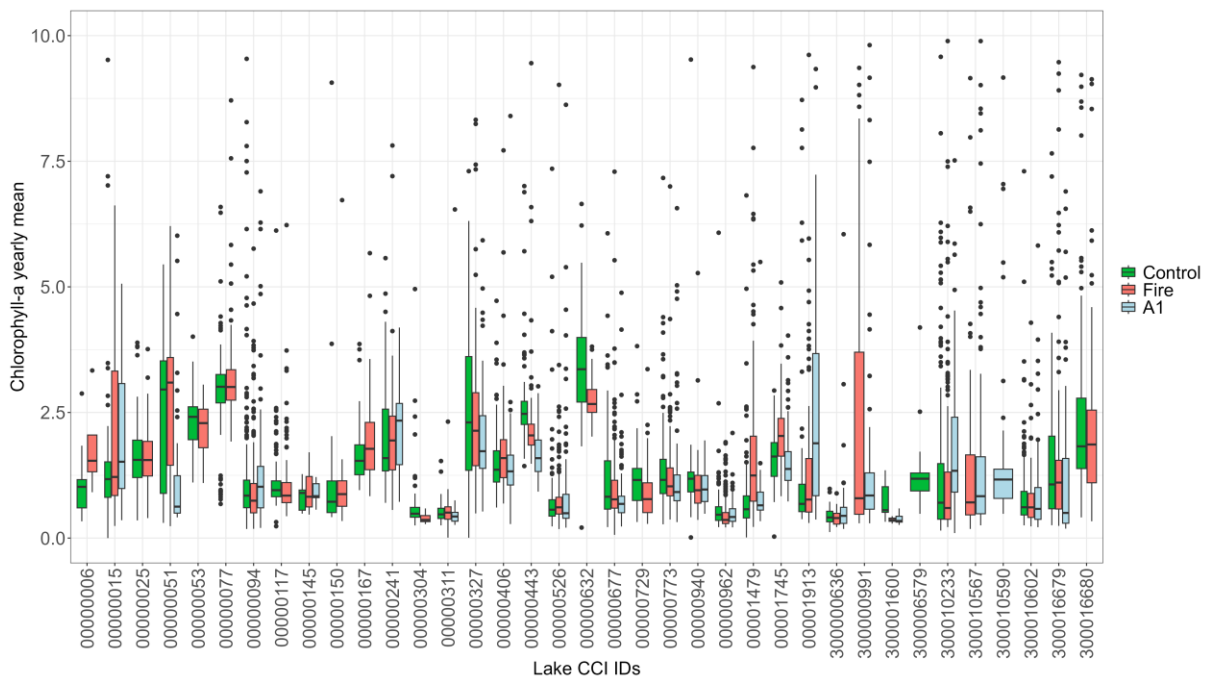


Figure 5-2. Boxplots of control (C, green), Fire (F, red) and post-fire (A1, light blue) weekly average Chl-a concentration (y-axis) for the pristine lakes under analysis (x-axis). In some cases, post-fire A1 year is not available, according to the method applied.

Comparing control (green) and fire (red) boxplots, we can observe that Chl-a annual mean concentration does not give a consistent response to fire event. It is likely that fires impact over

shorter time scales after the event and Chl-a annual average values are not significantly altered. More detailed statistical analysis is needed to focus on shorter time scale (seasonal, monthly, weekly) together with a time series approach.

5.2 Relationship between Chl-a daily anomalies and burned areas

In this part of the study, we present results on the analysis of the relationship between Chl-a anomaly and the amount of area burned within the lake catchment. For the pristine lakes identified at global level (n=234) we investigated the possible impact of fires on water quality by comparing trends of daily Chl-a anomaly and daily burned area. Anomalies in daily Chl-a were derived by satellite water colour measurements (Lakes_cci dataset) according to the methodology proposed by Wang et al. (2021).

Intersecting pristine lakes (n=234) with the HYDRObasin layer we obtained a total of 231 lakes to be further investigated. Then, we selected lakes and their connected catchment with BA>0 over the time period of interest (2001-2020) obtaining 74 lakes. Total BA was calculated for the whole lake catchment, build as reported in section 3.

Following the approach proposed by Wang et al. (2021), we derived two Chl-a anomaly products for each lake in the database: difference and ratio (or in its relative difference) both computed with respect to Chl-a climatology (*Chl-a Clim*). The Chl-a climatology layer is the Chl-a median value calculated for the 61 days preceding the Chl-a daily estimation; these climatology values are calculated on the first and fifteenth day of each month covering days 1-14 and days 15 to the end of the month, respectively. The 61-day *Chl-a Clim* data are calculated with a 15-day lag time to avoid anomalous Chl-a values that would significantly impact the Chl-a anomaly calculations for the period. As for other analysis, the calculation has been done for the two distinct periods: 2003-2011 (p1) and 2016-2020 (p2).

$$\Delta_{Chla} = Chla_{day} - Chla_{clim} \quad \text{Eq. 1}$$

Where Δ_{Chla} is the daily anomaly difference [mg m^{-3}], $Chla_{day}$ is the Chl-a concentration of a specific day and $Chla_{clim}$ is the 61-day Chl-a climatology value (one of the two values calculated for each month).

The Chl-a anomaly ratio (or relative difference) ($\Delta_{ratio_{Chla}}$) is calculated as follows:

$$\Delta_{ratio_{Chla}} = \Delta_{Chla} / Chla_{clim} \quad \text{Eq. 2}$$

with Δ_{Chla} from Eq 1, $\Delta_{ratio_{Chla}} \geq -1$, $\Delta_{ratio_{Chla}} = -1$ when $Chl-a=0 \text{ mg m}^{-3}$.

Then, we plotted the result time series of Chl-a anomalies with BA daily values for each lake and catchment and the two periods (p1 and p2).

A total of 148 graphs (2*74 lakes and catchments; Annex 2) were generated and inspected. When simultaneous high burned area and Chl-a anomaly was observed, further investigations were carried out on the identified lakes (Table 5-1) as follows:

1. Visualization in QGIS (3.16) of layers of lake area, catchment area and burned area maps (with DOY of burned pixel detection, and Land cover of the burned pixel) to identify the spatial and temporal occurrence of fires.
2. Plot of time series of Chl-a and Turbidity concentration in lake waters in the pre- and post-fire period.
3. Plot of the monthly precipitation (ERA5 dataset) and burned area in the year and the catchment under analysis.

Table 5-1. Lake's identification, characteristics (trophic state, altitude, area, maximum depth), year of the fire event to be investigated for fire effects on water quality and land cover of the burned area pixels are reported.

Lake_ID, Name	Trophic state (pre-2012)	Trophic status (post-2016)	Altitude (m a.s.l.)	Area (km ²)	Maximum depth (m)	Fire event	Land Cover (LC_CCI)
---------------	--------------------------	----------------------------	---------------------	-------------------------	-------------------	------------	---------------------

						- Year	
375, Lake Flathead (US)	Oligotrophic	Oligotrophic	882	510	50	2003	Tree cover, needleleaved, evergreen, closed to open (>15%); Shrubland
411, Lake Pyramid (US)	Oligotrophic	Oligotrophic	1157	487	107	2017	Shrubland
677, Lake Bear (US)	Ultra-oligotrophic	Ultra-oligotrophic	1806	280	29	2003	Shrubland
782, Lake Pasfield (Canada)	Ultra-oligotrophic	Oligotrophic	402	243	220	2010	Tree cover, needleleaved, evergreen, closed to open (>15%); Sparse vegetation (tree, shrub, herbaceous cover) (<15%)
1726, Lake Terewah/Narran (Australia)	Ultra-oligotrophic	Ultra-oligotrophic	118	267	6	2003	Tree cover, needleleaved, evergreen, closed to open (>15%); Mosaic tree and shrub (>50%) / herbaceous cover (<50%)
300010602, Lake Puelo (Argentina)	Ultra-oligotrophic	Ultra-oligotrophic	150	44	180	2015	Mosaic tree and shrub (>50%) / herbaceous cover (<50%); Tree cover, needleleaved, evergreen, closed to open (>15%);

In Figure 5-3 example plots of Chl-a anomaly (delta and delta-ratio) are reported with Chl-a climatology and burned area for Lake Flathead (US), Lake Bear (US), and Lake Terewah/Narran (AUS). For the three lakes, 2003 is evident as the year with high burned area followed by a high Delta-ratio Chl-a. For Lake Flathead and Lake Bear the delta ratio anomaly was of 3-6, while for Lake Terewah/Narran this value was over 100. The order of magnitude of the BA was much higher for the Lake Flathead (> 100 km²) compared to the other two lake catchments (~10-30 km²).

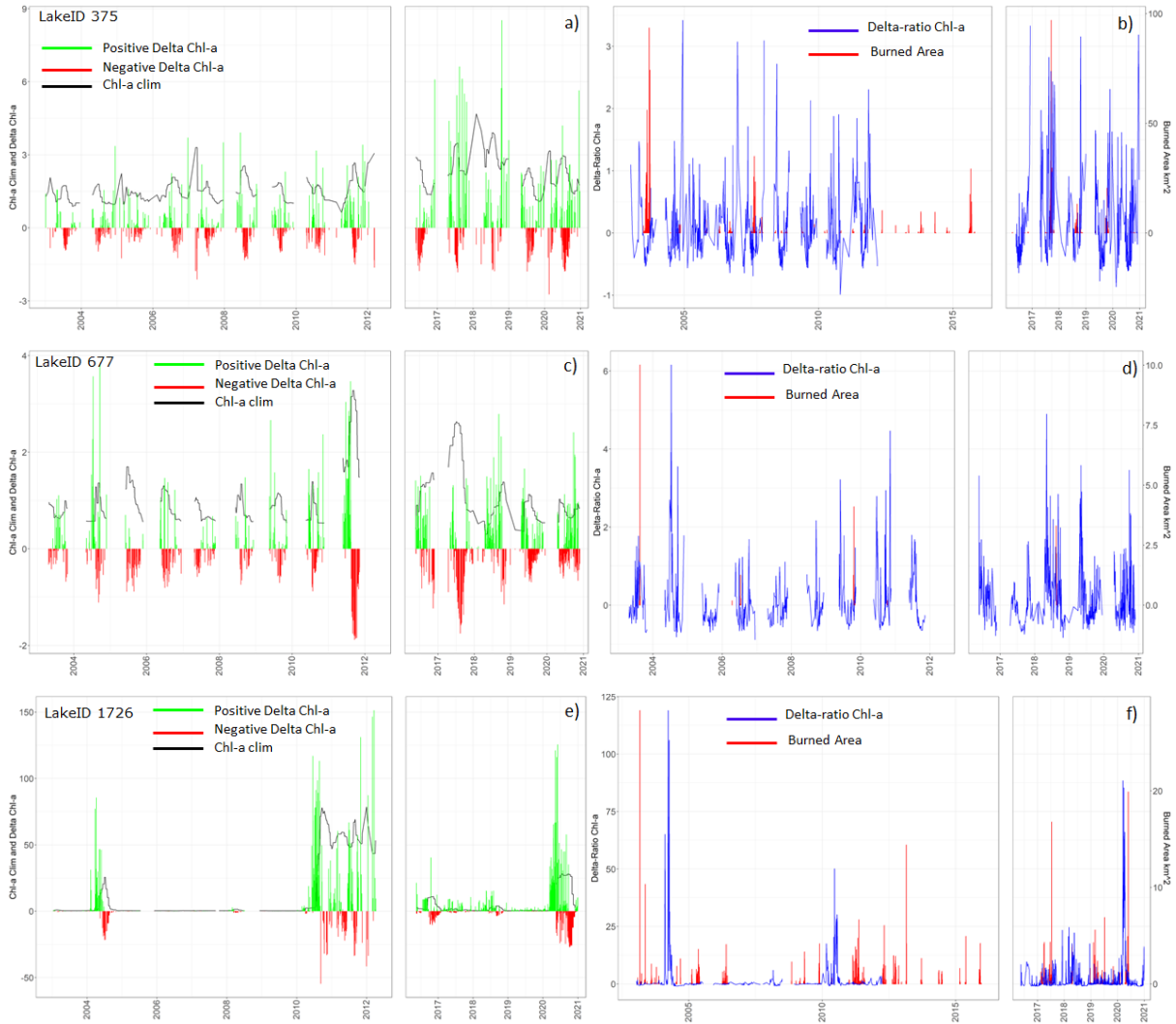


Figure 5-3. Plot of positive and negative Chl-a anomaly (Delta Chl-a) with Chl-a reference (Chl-a clim) (a, c, e), and plot of Chl-a anomaly ratio (Delta-ratio Chl-a) with burned area (b, d, f) for Lake Flathead (US; Lake_ID 375), Lake Bear (US; Lake_ID 677), and Lake Terewah/Narran (Australia; Lake_ID 1726), respectively.

In the Lake Pasfield catchment and at the same time period (p1: 2003-2011), the year 2010 was characterized by high total BA (~50 km²) and followed by a delta-ratio Chl-a >3 (Figure 5-4).

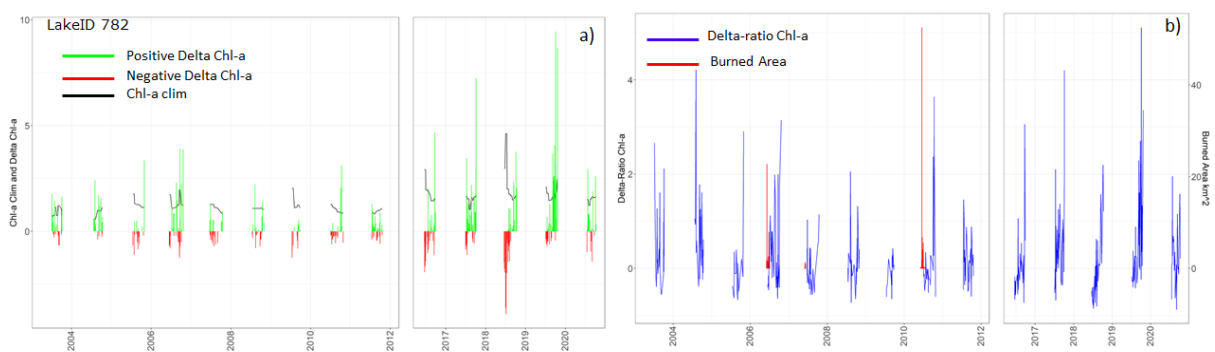


Figure 5-4. Plot of positive and negative Chl-a anomaly (Delta Chl-a) with Chl-a reference (Chl-a clim) (a), and plot of Chl-a anomaly ratio (Delta-ratio Chl-a) with burned area (b) for Lake Pasfield (Canada; Lake_ID 782).

Two other cases were identified for the second period of analysis (p2: 2016-2020): Figure 5-5 Lake Pyramid (US) and Lake Puelo (RA) where an elevated BA was detected in 2017 (>120 km²) and 2016 (>30 km²), respectively, for the two catchments and lake waters were characterized by Delta-ratio Chl-a >5 and >20, respectively (Figure 5-5).

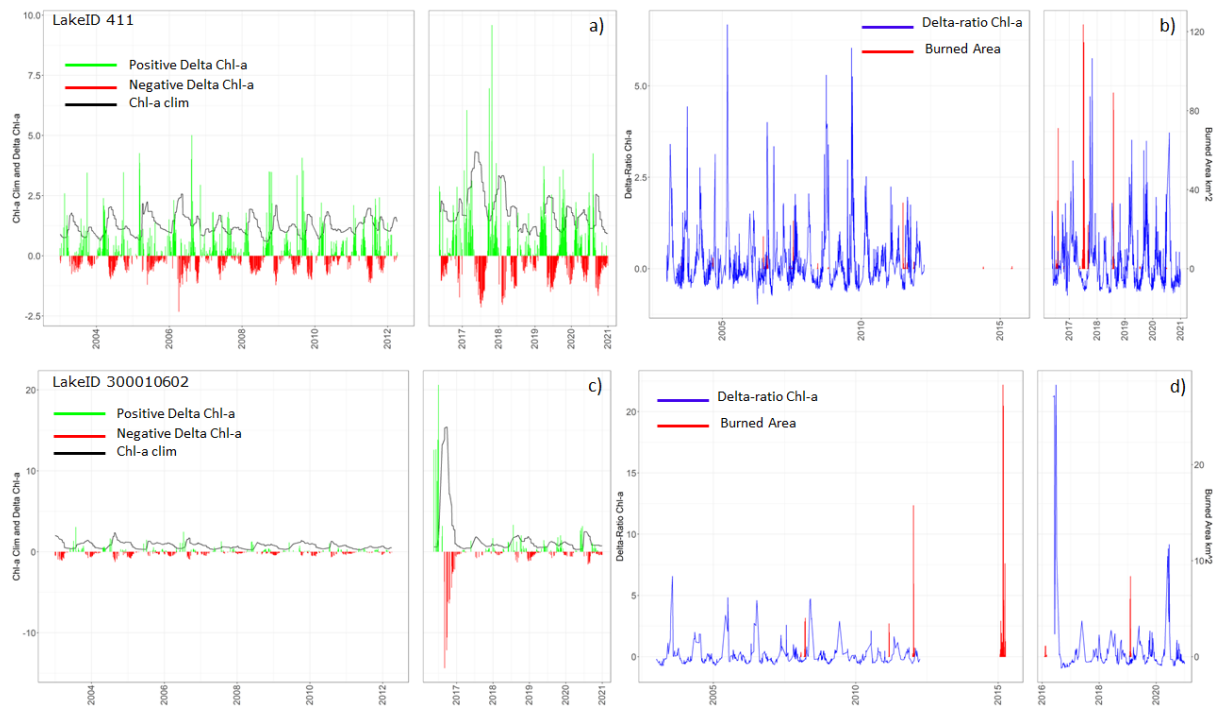


Figure 5-5. Plot of positive and negative Chl-a anomaly (Delta Chl-a) with Chl-a reference (Chl-a clim) (a, c), and plot of Chl-a anomaly ratio (Delta-ratio Chl-a) with burned area (b, d) for Lake Pyramid (US; Lake_ID 411) and Lake Puelo (Argentina; Lake_ID 300010602), respectively.

For the above-mentioned lakes, we also analysed maps of burned areas over the lake catchment area to identify timing of major fire events (DOY of burned pixel detection). Temporal trend of Burned Areas was plotted with Chl-a (and Turbidity) concentration and total precipitation (tp), for the period investigated for each lake.

For example, in Lake Flathead (US) burned areas were detected between July and September 2003. Chl-a values show a similar pattern in spring 2003 and 2004, while it can be noticed a slightly lower Chl-a concentration in the summer period of 2002 and 2003 compared with 2004 (post-fire) with a similar precipitation pattern among the years (Figure 5-6). An example of Chl-a concentration maps for summer 2003 and 2004 are reported in Figure 5-7, where this pattern is clearly evident.

In Lake Terewah/Narran (AUS) catchment, fire events occurred from March to October 2003. In mid of July of the same year a peak of Turbidity (43 NTU) was estimated for the shallow lake waters, followed by a peak in Chl-a concentration (>30 mg m⁻³) in April 2004 preceded by intense rainfall events (Figure 5-6). In Turbidity concentration maps for the period pre- and post-fire 2003, and Chl-a concentration maps for the period March-April 2004 (Figure 5-8).

Instead, for Lake Bear (ID_677; US) and Lake Pasfield (ID_782; Canada) were not identified differences between pre- and post-fire events (of the period 2003-2012) in Chl-a and Turbidity concentration patterns (Figure in Annex 2).

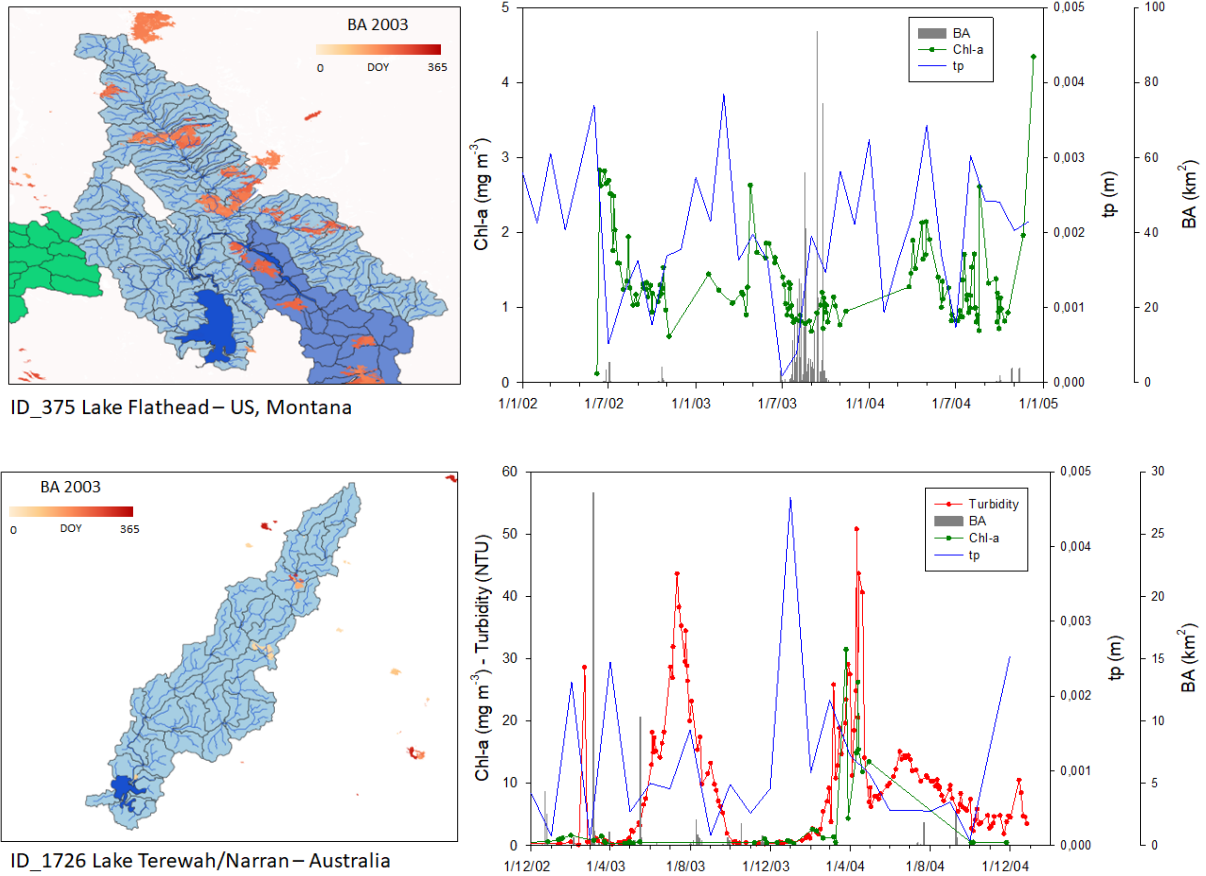


Figure 5-6. Maps of Lake Flathead (upper panel) and Lake Terewah/Narran (lower panel) with their catchments and burned area (BA) distribution and occurrence (DOY). The graphs report Chlorophyll-a (Chl-a, green) and Turbidity (red) concentrations, total precipitation (tp, blue) and BA histograms (gray).

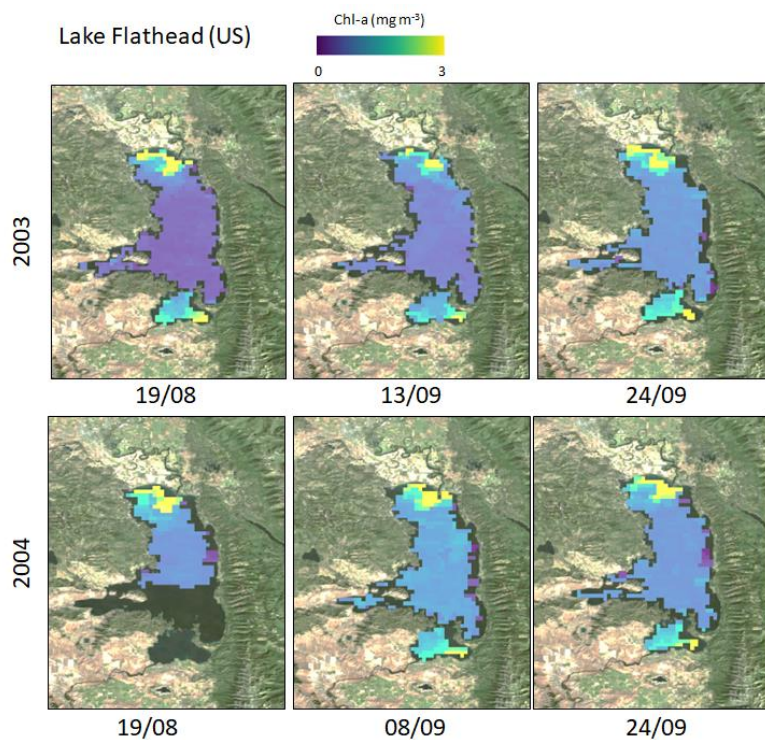


Figure 5-7. Chlorophyll-a maps of Lake Flathead (ID_375; US) in the summer 2003 and 2004, that is immediately after and one year after the fire events. Fires occurred in March and September 2003.

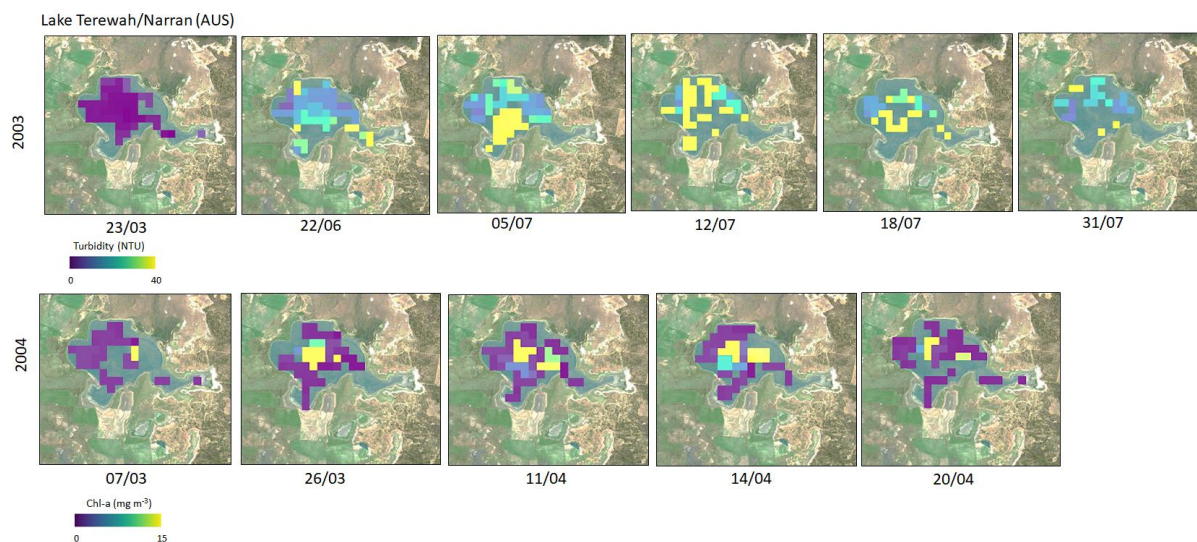


Figure 5-8. Turbidity and chlorophyll-a maps of Lake Terewah/Narran (ID_1726; AUS) in the pre- and post-fire period of 2003 and a year after the fire in 2004, respectively. Fires occurred from March to October 2003.

Lake Pyramid (US) and Lake Puelo (AR) showed an interesting response of lake water Chl-a concentration values after fire events. In Lake Pyramid catchment, large burned areas were detected between July and September 2017, and a peak of Chl-a (up to 11 mg m^{-3}) was estimated at the end of October of the same year after a period of low precipitation (Figure 5-9). Maps of Chl-a concentration for this post-fire period are reported in Figure 5-10.

In Lake Puelo, the greatest fire events observed for the 18-year period covered by this study occurred between March and April 2015 (up to 100 km^2). A Chl-a peak (7 mg m^{-3}) was recorded in September 2016 after a period of high variability in precipitation (Figure 5-9). However, there are no Chl-a data available from 2015 to May 2016. In Figure 5-10, maps of Chl-a concentration for the period post-fire are reported. This anomalous year in terms of fire (2015) could explain the difference in the median Chl-a reference data of 2016 (see Figure 5-5c), but further investigations are needed.

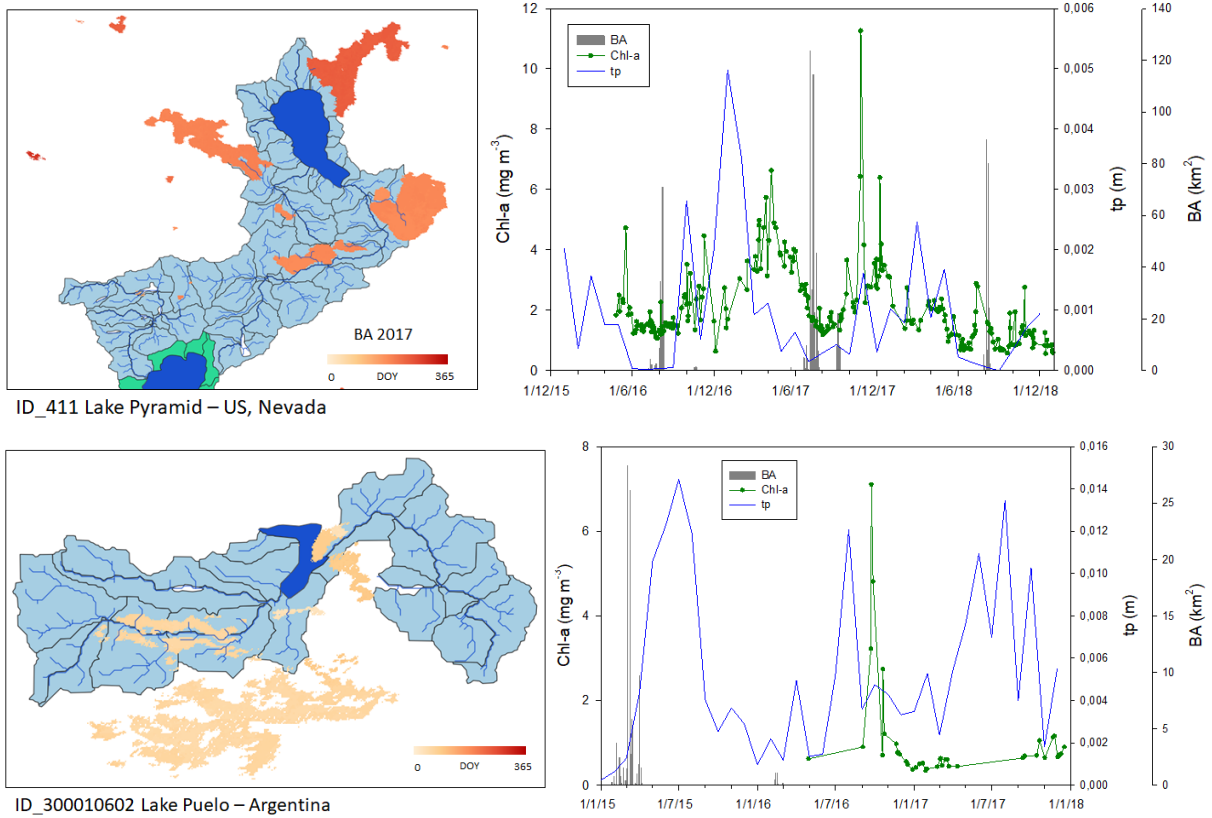
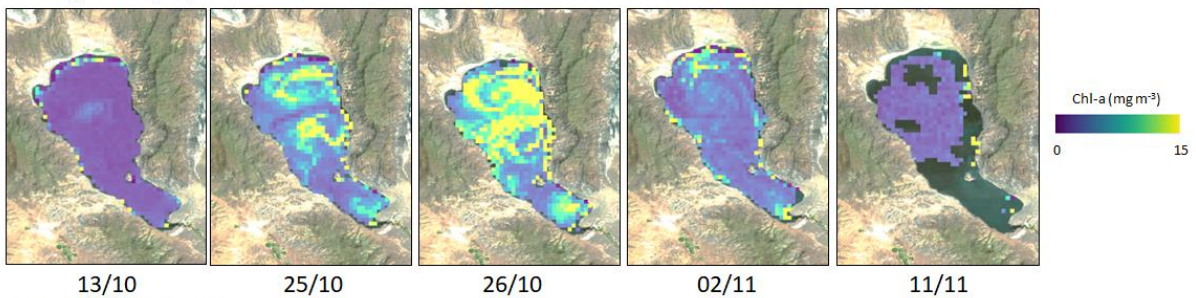


Figure 5-9. Maps of Lake Pyramid (ID_411) (upper panel) and Lake Puelo (ID_300010602) (lower panel) with their catchments and burned area (BA) distribution and occurrence (DOY). The graphs report Chlorophyll-a (Chl-a, green) concentrations, total precipitation (tp, blue) and BA histograms (gray).

Lake Pyramid (US) - 2017



Lake Puelo (AR) - 2016

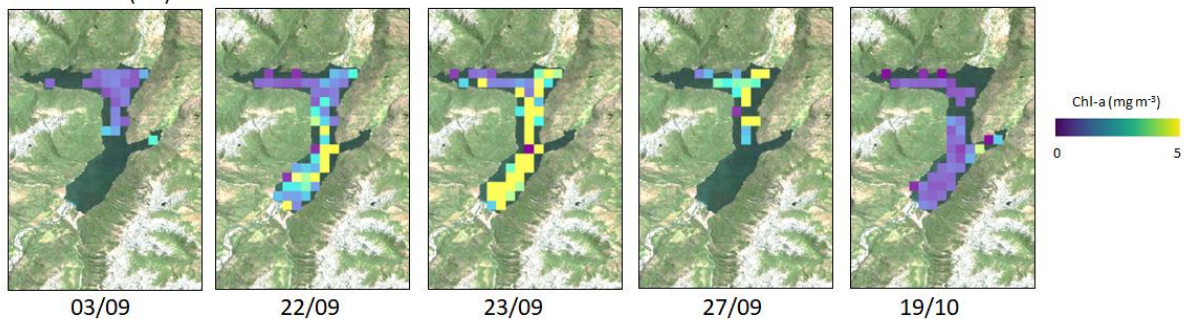


Figure 5-10. In the upper panel chlorophyll-a maps of Lake Pyramid (ID_411; US) in the season following fire events of 2017. Fires occurred between July and September 2017. In the lower panel Chl-a maps of Lake Puelo (ID_300010602; AR) in the post-fire period of 2016. Fires occurred in March and April 2015.

In conclusion, from these analyses, we can summarize that in some lakes investigated a Chl-a increase is likely a response to fire events and subsequent runoff from the catchment to the receptor lake. The distribution of burned area were close to the lake surfaces and the maximum burned area per day was comprised between 30 and 120 km². The land cover of burned pixels was comparable between the case selected, that is tree cover, mosaic tree and shrub, and herbaceous cover. The Chl-a concentration (lake average value) response in lake waters was detected with a different time span, from short to medium term: after one-two months (e.g., lake Pyramid) or in the following 10-12 months (e.g., lake Flathead, Lake Terewah/Narran and Lake Puelo). Finally, only in the shallow Lake Terewah/Narran a possible response by both Turbidity and Chl-a values occurred after few months for the former, and after one year for the latter. This latter case is in agreement with the finding of Uzun et al. (2020), that observed that three fires that occurred in the Northern California Coastal Ranges in 2015 evidenced high levels of turbidity, and total suspended solids during the first rainy season postfire. In addition, Rust et al. (2019) found that increased nitrogen, phosphorus and cation exports were common the first 5 post-fire years from a synthesis of 159 wildfires across the western United States. The other lakes of our study with a medium-term Chl-a increase response are likely in agreement with the finding of this latter study.

6. Investigation of WFD priority substances data for assessing wildfire impacts on lakes

6.1 Background

Polycyclic aromatic hydrocarbons (PAHs) are a group of ring-structured organic compounds, introduced into the environment mainly via anthropogenic or natural combustion processes. Anthropogenic sources include combustion of fossil fuels, commercial and industrial heating systems, incinerators, industrial discharges, runoff from roads, while natural combustion processes include wildfires.

PAHs are transported in the atmosphere and can reach the water environment following wet and/or dry depositions. During rainfall events, a significant load of PAHs can be transported from the terrestrial surface into water bodies by runoff, resulting in non-point source pollution and jeopardizing aquatic ecosystems (Zheng et al., 2012). Contaminant loading associated with stormwater runoff from recently burned areas is poorly understood, even though it has the potential to affect downstream water quality. Stein et al. (2012), assessing regional patterns of runoff and contaminant loading from wildfires in urban fringe areas of southern California found that polycyclic aromatic hydrocarbon flux was four times greater from burned areas than from adjacent urban areas. PAHs have low water solubility and tend to associate with suspended particles in water, settling on bottom sediments where they may persist. They are potentially dangerous in waters even at very low concentrations due to their bioaccumulation along the aquatic food chain; with high toxicity, mutagenicity and potential carcinogenicity they represent a threat for wildlife and human health (Gorshkov et al., 2019).

Polycyclic aromatic hydrocarbons are present in all types of waters and were included in the list of stable organic pollutants (SOP) by the Stockholm Convention (2001). In Europe polycyclic aromatic hydrocarbons are classed as priority hazardous substances and ubiquitous persistent, bioaccumulative and toxic (uPBT) compounds under the Water Framework Directive (WFD-2000/60/EC) in the field of water policy. The related Directive 2008/105/EC and Directive 2013/39/EU set environmental quality standards (EQS) for priority substances including PAHs in water and biota. uPBT substances persist in the environment, can be transported long distances and pose long-term risks to human health and ecosystems. Owing to widespread environmental contamination, achieving concentrations at or below the EQS for this group of substances can be particularly challenging (European waters Assessment of status and pressures, Report 2018).

European member states are required to report on priority substances in the aquatic environment. These include PAHs such as anthracene, benzo[b]fluoranthene, benzo[k]fluoranthene, benzo[a]pyrene, benzo[ghi]perylene, indeno[1,2,3-cd]pyrene, naphthalene and fluoranthene. The reporting frequency is one year of monthly sampling every six years, for every river basin management plan (six years cycle).

European Member States reported their data to the Water Information System for Europe (WISE). We have explored the WISE database (<https://www.eea.europa.eu/data-and-maps/data/waterbase-water-quality-icm-2>) in order to match instances of significant fires with available monthly records of PAHs in lakes and key events have been analysed.

Detection of changes in PAHs concentrations in lakes, not subjected to other significant anthropogenic pollution, could be used to confirm an impact of wildfires and help pinpoint lakes and periods for more detailed examination using Lakes_cci data.

The lowest molecular weight studied PAHs (naphthalene, fluorene, phenanthrene, anthracene, fluoranthene and pyrene) appear to be the major ones produced by forest fires (Vergnoux et al., 2011) and were predominant in rivers after forest fires (Olivella et al., 2006). In particular, it is expected that fire events could be identified by increases in the runoff from burnt areas and in lake water of fluoranthene and naphthalene relative to other PAHs (Campos et al., 2012; Gorshkov et al., 2021).

In this study, periods when we identified a temporal match between fire occurrence and PAHs increase in lake waters have been examined also for changes in lake water Chl-a and Turbidity to understand wider ecological and system implications. The output has featured examples within the

context of Lakes_cci matching available PAHs data in the Water Framework Directive (2000/60/EC) reporting WISE database.

6.2 Methods

The procedure we applied for investigating potential fire effects on PAHs concentrations in lake water in Europe, was based on merging the Lakes_cci dataset with European reporting WISE dataset.

European lake water monitoring stations from the WISE *WATERBASE* database (<https://www.eea.europa.eu/data-and-maps/data/waterbase-water-quality-icm-2>) were downloaded and matched with those included in the Lakes_cci project (using the Version 2.0.2 shapefile). For matching stations, data from in-situ monitored physico-chemical parameters and dangerous substances in *WATERBASE* were extracted. The chemistry data was then filtered for parameters typically affected by fires. In particular, a list of PAHs within monitored dangerous substances (Fluoranthene Naphthalene, Benzo(a)pyrene, Benzo(b)fluoranthene, Benzo(k)fluoranthene, Benzo(g,h,i)perylene, Indeno(1,2,3,cd)pyrene) were considered.

Utilizing QGIS software, the extension of burned areas (FireCCI51 dataset) and fire events were overlapped with matches of Lakes_cci and WISE monitored lake stations for PAHs. Investigations were carried out on time-series to detect the variation in PAHs concentrations in lakes positioned near burned areas and fire events.

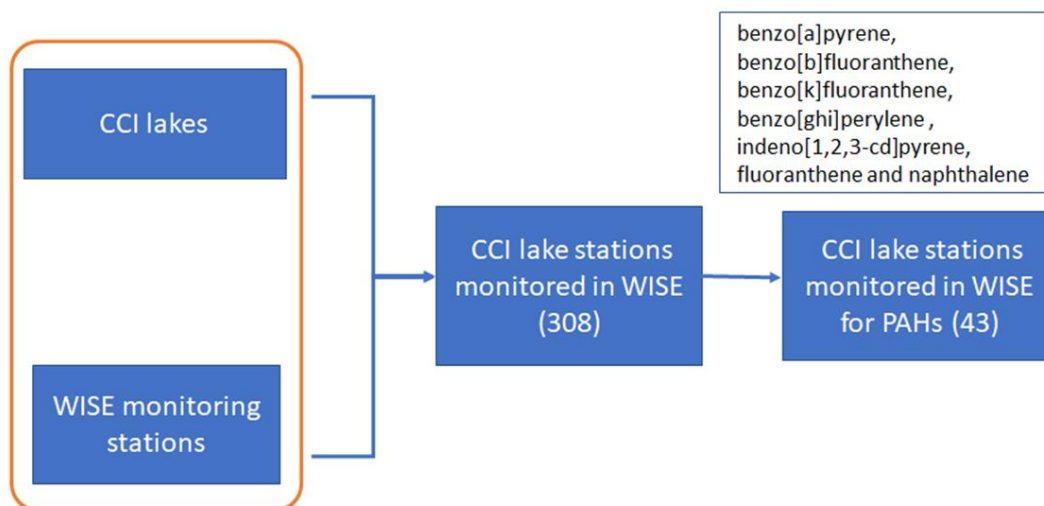
PAHs concentrations were compared with the environmental quality standards (EQS) for priority substances according to the Directive 2013/39/EU.

6.3 Results

A total of 308 lake stations were found in common between Lakes_cci and WISE monitored lakes (Figure 6-1). According to the WISE dataset utilized for this analysis, eleven European countries have reported PAHs concentration in lake water, with a total of 43 common lake stations, corresponding to 25 lakes (Figure 6-1).

The frequency of the data available varied among member states, from twelve to one sample per year with one country reporting annually and other countries reporting for one year out of every six as mandated by the WFD.

The investigation of the PAHs listed, within the WISE dataset, revealed few cases of increased concentrations in lake waters. The following two lake cases have been selected since the increases in PAHs arose in comparable periods of time and in nearby areas of wildfires occurrence.



● CCI lake stations monitored in WISE

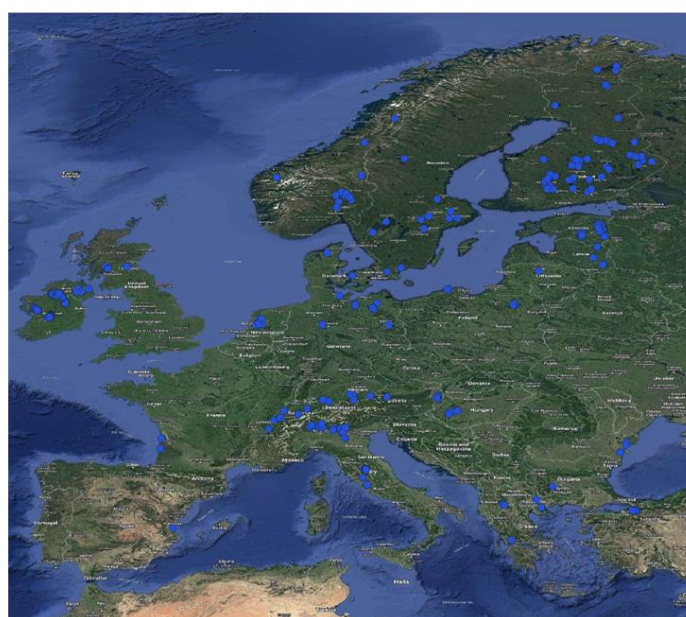


Figure 6-1. Scheme of the approach used to merge the Lakes_cci dataset with European reporting WISE dataset. The number reported in brackets refers to the number of lake stations obtained as output.

Case 1. Lake Corrib (Ireland; Lakes_cci ID 1057)

Lake Corrib is one of the largest lakes in Ireland, with a surface area of 176 km² and a maximum depth of 51 m. Situated in the west of the country (Figure 6-2), it is an oligotrophic lake (EPA data Chl-a 1.5-2.5 µg L⁻¹) and classified in good ecological and chemical status according to the Water Framework Directive (60/2000) classification.

Regarding PAHs concentration patterns, during 2016 we detected an increase in Fluoranthene and Benzo(a)pyrene concentrations in May 2016 (Figure 6-3). However, concentrations measured for both substances were below the MAC-EQS (maximum annual concentration - Environmental Quality Standards) set by the Directive EC 2013. Lakes_cci water quality products for this lake revealed an increase in Chl-a concentration and partially in water Turbidity in the same month of May 2016. These results were confirmed by chlorophyll-a in situ data reported in the WISE dataset, with the highest concentrations of the period 2013-2020 measured during summer 2016.

A fire was detected in 2016, with 5 km² of total burned area, at 3 km distance from the lake, during the period 23 April-15 May 2016. Land cover type burned was mainly shrubs or herbaceous cover flooded (code 180), mosaic trees, shrubs and herbaceous (code 100), and sparse vegetation (code 150).

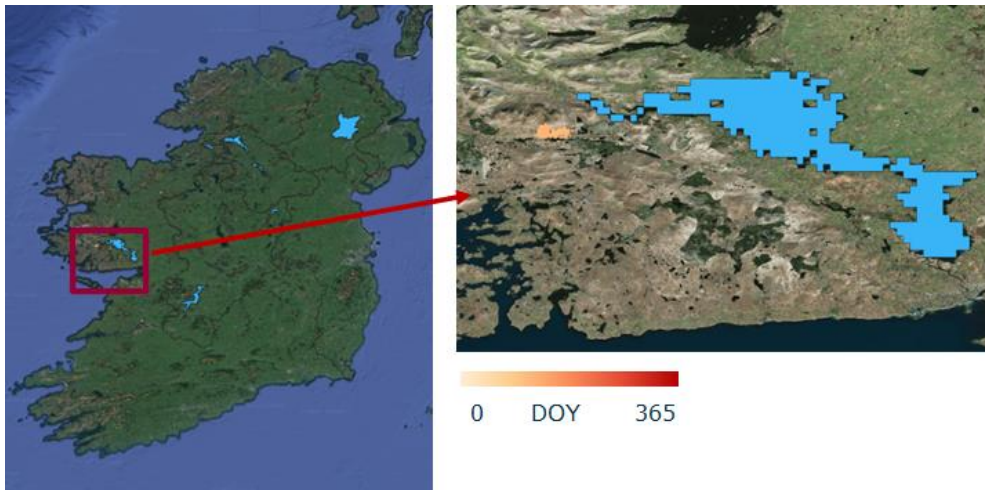


Figure 6-2. Lake Corrib (IE) location and fire site active during May 2016 (DOY of burned pixel detection).

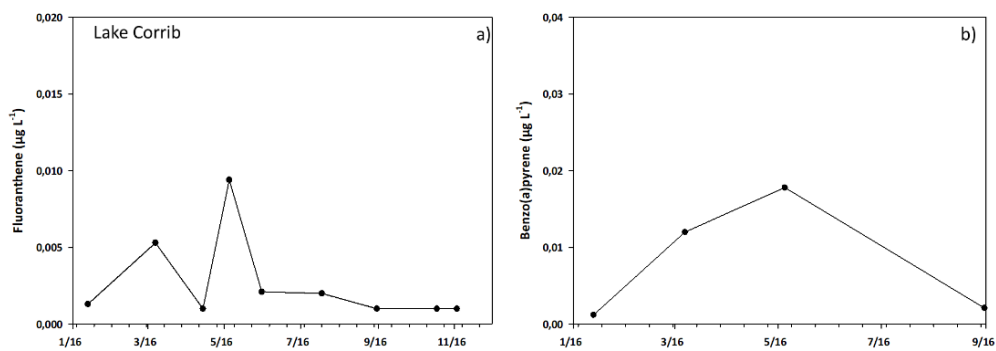


Figure 6-3. Fluoranthene and Benzo(a)pyrene concentration in 2016 in Lake Corrib.

The wind diagram below, calculated for the same period of the fire occurrence utilizing ERA5 datasets, indicates the strongest winds occurred along south-west north-east direction, suggesting a potential transport of burned material and contaminants from the fire site to the lake surface.

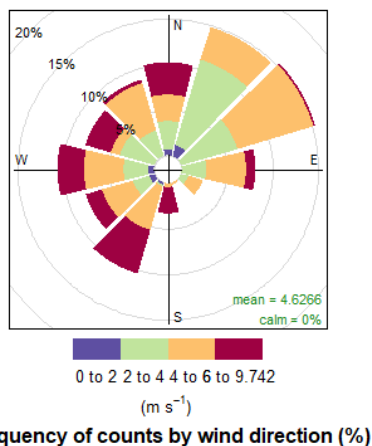


Figure 6-4. Wind diagram for the period April-May 2016 around Lake Corrib.

Case 2. Lake Batak (Bulgaria; Lakes_cci ID 300014434)

Lake Batak is a reservoir located in the Rhodope Mountains, at 1107 m of altitude and is the third largest lake in Bulgaria, with a surface of 22 km² and a maximum depth of 35 m. According to Belkinova and Gecheva (2013), it is designed as heavily modified water body in oligotrophic conditions.

Data available for PAHs during 2018-2019 indicated an increase, from background concentrations, of fluoranthene and naphthalene (Figure 6-5). Those increases started to be detected during summer 2018, with higher concentrations reported during autumn and winter 2018/2019. Concentrations measured were below the MAC-EQS (maximum annual concentration- Environmental Quality Standards) set by the Directive EC 2013. Lakes_cci water quality products for this lake revealed a peak in Chl-a concentration and in water Turbidity in August 2018.

Different fires were detected during 2018, in particular during the periods of end of June-8 July and end of September-10 November 2018. As showed in Figure 6-6, the fires were located at north-east of Lake Batak, at a distance of 16 to 45 km. Land cover burned was cropland (20), mosaic cropland and natural vegetation- trees shrubs, herbaceous (30 and 40).

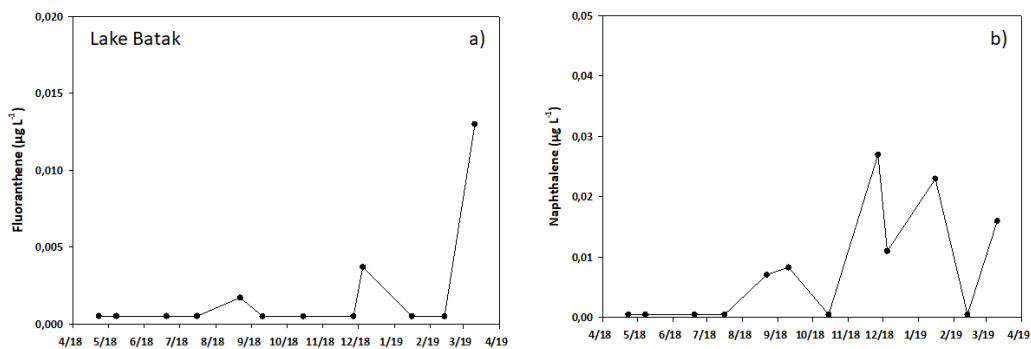


Figure 6-5. Fluoranthene and Naphthalene concentration in 2018/2019 in Lake Batak.

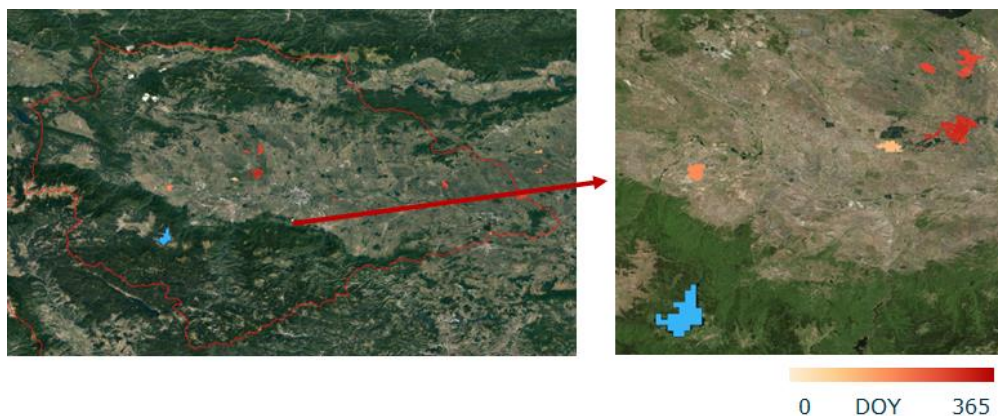


Figure 6-6. Lake Batak (BG) location and fire site active during 2018 (DOY of burned pixel detection).

The wind diagrams, calculated for the same periods of the fire occurrences utilizing ERA5 datasets, indicate that deposition by wind in the first period was unlikely, while during the second period considered there was potential for airborne deposition to the lake (Figure 6-7).

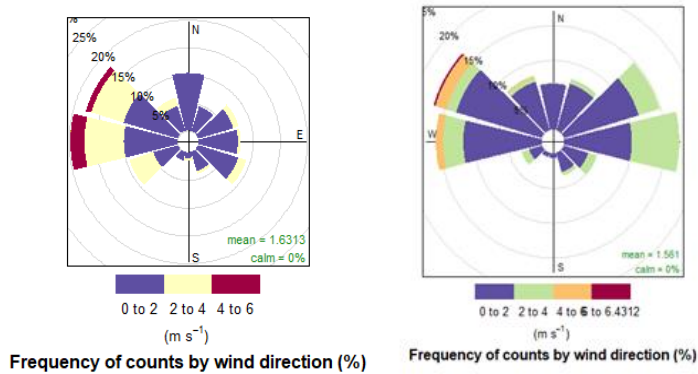


Figure 6-7. Wind diagrams for the summer and autumn period of fires in 2018 around Lake Batak.

In conclusion, examining the concurrence of fires and increases in PAHs in lakes confirms a link between wildfires and lakes through either airborne or fluvial transport. However, the data available for exploration were limited. This is because there was a limited match between Lakes_cci and European lakes reported to WISE for these contaminants coupled with the added complication of often infrequent fires having to coincide with the one in six years monitoring strategy employed by the European directive. Nevertheless, for a few lakes we could demonstrate causal links which is demonstrative of what could be achieved with a more comprehensive and joint-up monitoring programme.

7. Conclusions

The main objective of this study was to evaluate the effects of wildfires on lake water quality, with particular focus on pristine lakes at regional and global scale. We used ESA CCI Fire and Lake ECVs with other global products (i.e., ERA5 precipitation and wind) to assess changes in lake water quality due to wildfires and the effects across the riverine network to the receptor lake.

We based the analysis on an innovative model/criteria, which defines how lake sub-basins are connected to each other, allowing a better identification of runoff patterns from burned areas to lake basins.

We applied four main approaches for this study:

- i) Source-pathway-receptor (SPR) model to select lakes most susceptible to fire impacts
- ii) Correlation between fire occurrence and water quality on ultra- and oligotrophic lakes
- iii) Analysis of Chl-a anomalies in ultra- and oligotrophic lakes
- iv) Analysis of PAHs to investigate the impact of wildfires on European lakes

In this report, we first briefly reported the criteria of the SPR approach and then we examined major results of this methodology. A previous analysis provided a selection of candidate lakes likely affected by wildfires via riverine inputs. The selected lakes had a high SPI (standardised precipitation index, >1.5) and a high (>30) ratio of catchment area/lake area. This ratio is indicative of the effective surface over which terrestrial nutrients are collected by inflowing waters that ultimately reach the lake. About 20 lakes showed a clear response to a temporal succession of fire occurrence, precipitations and changes in water quality conditions (chlorophyll-a and/or turbidity).

Considering pristine lakes (in ultra- and oligotrophic status), we analysed the correlation between fire occurrence and water quality by comparing *fire* and *no fire* periods. The objective of this analysis was to assess whether, for each lake, we could observe a significant difference of average annual Chl-a in fire-free years preceding an event and in the 1/2 following years. To this aim, we defined a set of conditions on temporal occurrence of fire to subset the whole dataset of pristine lakes and to extract lakes with control years (absence of fires). For this subset, and at annual level, we did not find a significant difference in average Chl-a concentration between pre- and post-fire periods. However, examining the responses of individual lakes, we observed site-specific responses with positive (increase), negative (decrease) and null (similar) changes of Chl-a for pre-fire, fire and post-fire years. It is likely that fire events could impact lake water quality over a time scale shorter than the year; a more detailed analysis is needed considering shorter temporal scale, such as seasonal, monthly and weekly frequency. This analysis could be also carried out using approaches specifically developed for modelling time series trends and time series correlation.

In the third point, we analysed the relationship between daily Chl-a anomaly and the amount of area burned within the lake catchment for pristine lakes. The main outcome was that less than 10% of pristine lakes investigated showed an increase in Chl-a concentration after one year from a wildfires event, while no changes in turbidity were detected.

For the last activity, we examined the concurrence of fires and increases in PAHs in lakes, as a step to confirm a link between wildfires and water quality changes, either through airborne or fluvial transport. Although data available were limited, because matches between Lakes_cci and European lakes reported to WISE for these contaminants were scarce and infrequent, a couple of lakes demonstrated causal links and perhaps could be demonstrative of what could be achieved with a more comprehensive monitoring programme. Further work within the Lakes_cci project could explicitly include more lakes that are subject to high quality monitoring programmes by national agencies to maximise cross agency opportunities enabling multiple synergies to be capitalised upon.

Pristine lakes are under threat globally, with lakes in remote areas now facing growing threats from climate change, including the increased incidence of wildfires. In this study we expected to find more evident responses to wildfires in oligotrophic lakes, due to the input of nutrients released during wildfires via direct airborne deposition or from runoff. This is because of the numerous studies in scientific literature documenting increases of primary production in response to wildfires in oceans, where water nutrients levels are comparable to those in oligotrophic lakes. Moreover, in lakes the changes of water conditions might be affected by a larger number of variables than in oceans. We

found a response in Chl-a to fire only in a limited number of oligotrophic lakes probably due to the complexity of lake ecosystem structure and function. Physico-chemical and biological features of lakes and their catchment characteristics influence ecosystem primary production responses in the receptor lake.

Nutrient inputs from wildfires to lakes may have resulted in promoting an increase in phytoplankton biomass, but the increase in Chl-a concentration might have been limited and not effectively observable in global EO products, given the already low initial concentrations in the lake. Moreover, when the fire response analysis considered average values over the whole surface lake, there might be a chance of failing in capturing the complexity of spatial heterogeneity and to identify local Chl-a variations.

We also found responses to wildfires for lakes with a higher trophic level (e.g., mesotrophic lakes), suggesting the opportunity to further investigate responses in these lakes. While the trophic status of lakes is important for pre-fire conditions, in lakes with higher nutrient values tending to dampen the effect of fire-mediated inputs, lake responses must be considered in combination with other factors such as the morphology of the surrounding landscape, lake depth and the ratio catchment/lake areas. A more comprehensive ecological assessment of the studied lakes would be favourable (e.g., nutrients). Further work can exploit the Chl-a anomalies approach or the correlation between fire occurrence and water quality (fire period vs no fire period) to investigate the Chl-a response in mesotrophic lakes.

The criteria for lakes trophic state classification utilized in this study (OECD, 1982) may have overestimated the number of lakes above oligotrophic conditions and may be too strict when applied to satellite measurements of Chl-a in lakes. Higher upper limits or a selection of boundaries between oligotrophic and mesotrophic conditions, for different lake typologies, may be beneficial and result in more lakes to be investigated for wildfires effects. Our choice of the OECD classification had the advantage of being applicable for different lake typologies at global scale.

In conclusion, this study included various approaches for the investigation of the effects of wildfires on lake water quality and contributed to a better understanding of their potential impacts on lake ecosystems. Due to the complexity of interactions including vegetation, soil, topography, hydrology, climate, and atmosphere, effects of burning on lake waters is likely to be highly site specific. Modelling the relationships between spatio-temporal patterns of burned areas and water quality due to wildfire impacts in aquatic environment remains a challenge.

8. References

- Belkinova, D. & Gecheva, G. (2013). Biological analysis and ecological status assessment of Bulgarian surface water ecosystems. Plovdiv University Publishing House, Plovdiv (Bg).
- Brown, K. P., Gerber, A., Bedulina, D., and Timofeyev, M. A. (2021). Human impact and ecosystemic health at Lake Baikal. *Wiley Interdisciplinary Reviews: Water*, 8(4), e1528. doi:10.1002/wat2.1528
- Campos I., Abrantes N., Vidal T., Bastos A. C., F. Goncalves F, Keizer J. J. (2012) Assessment of the toxicity of ash-loaded runoff from a recently burnt eucalypt plantation. *Eur J Forest Res*, 131:1889-1903
- Cannon, S. H., Gartner, J. E., Wilson, R. C., Bowers, J. C., & Laber, J. L. (2008). Storm rainfall conditions for floods and debris flows from recently burned areas in southwestern Colorado and southern California. *Geomorphology*, 96(3-4), 250-269
- Carrea, L., Crétaux, J. F., Liu, X., Wu, Y., Calmettes, B., Duguay, C. R., ... & Albergel, C. (2023). Satellite-derived multivariate world-wide lake physical variable timeseries for climate studies. *Scientific Data*, 10(1), 30
- CEC (Council of the European Communities) 2013. Directive 2013/39/EU of the European Parliament and of the Council, Official Journal of the European Union, 226/1, 17 p.
- CEC (Council of the European Communities), 2000. Directive 2000/60/EC of the European Parliament and of the Council, Official Journal of the European Union, 72 p.
- Chuvieco, E., Roteta, E., Sali, M., Stroppiana, D., Boettcher, M., Kirches, G. et al., (2022). Building a small fire database for Sub-Saharan Africa from Sentinel-2 high-resolution images. *Science of the total environment*, 845, 157139
- Dahm, C. N., Candelaria-Ley, R. I., Reale, C. S., Reale, J. K., & Van Horn, D. J. (2015). Extreme water quality degradation following a catastrophic forest fire. *Freshwater Biology*, 60(12), 2584-2599
- Edwards, D. C. and McKee T. B. (1997). Characteristics of 20th century drought in the United States at multiple time scales. *Climatology Report 97-2*, Department of Atmospheric Science, Colorado State University, Fort Collins, Colorado
- ESA. Land Cover CCI Product User Guide Version 2. Tech. Rep. (2017). Available at: maps.elie.ucl.ac.be/CCI/viewer/download/ESACCI-LC-Ph2-PUGv2_2.0.pdf
- European waters Assessment of status and pressures 2018. EEA Report No 7/2018. ISSN 1977-8449
- Giglio, L., Loboda, T., Roy, D. P., Quayle, B., and Justice, C. O. (2009). An active-fire based burned area mapping algorithm for the MODIS sensor. *Remote sensing of environment*, 113(2), 408-420
- Gorshkov A. G., Izosimova O. N., Kustova O. V. (2019). Determination of Priority Polycyclic Aromatic Hydrocarbons in Water at The Trace Level. *Journal of Analytical Chemistry*, 74, 771-777
- Gorshkov, A.G.; Izosimova, O.N.; Kustova, O.V.; Marinaite, I.I.; Galachyants, Y.P.; Sinyukovich, V.N.; Khodzher, T.V. (2021). Wildfires as a Source of PAHs in Surface Waters of Background Areas (Lake Baikal, Russia). *Water* 2021, 13, 2636. <https://doi.org/10.3390/w13192636>
- HydroSHEDS. 2014. «HydroBASINS». 2014. <https://www.hydrosheds.org/products/hydrobasins>
- Järvinen, M., S. Drakare, G. Free, A. Lyche-Solheim, G. Phillips, B. Skjelbred, U. Mischke, I. Ott, S. Poikane, & M. Søndergaard, 2013. Phytoplankton indicator taxa for reference conditions in Northern and Central European lowland lakes. *Hydrobiologia* 704: 97-113
- Lehner, Bernhard, e Günther Grill. 2013. «Global River Hydrography and Network Routing: Baseline Data and New Approaches to Study the World's Large River Systems: GLOBAL RIVER HYDROGRAPHY AND NETWORK ROUTING». *Hydrological Processes* 27 (15): 2171-86. <https://doi.org/10.1002/hyp.9740>
- Liu, D., Zhou, C., Keesing, J. K., Serrano, O., Werner, A., Fang, Y., et al. (2022). Wildfires enhance phytoplankton production in tropical oceans. *Nature communications*, 13(1), 1-9. doi:10.1038/s41467-022-29013-0

- Lizundia-Loiola, J., Otón, G., Ramo, R., and Chuvieco, E. (2020). A spatio-temporal active-fire clustering approach for global burned area mapping at 250 m from MODIS data. *Remote Sens. Environ.* 236, 111493. doi:[10.1016/j.rse.2019.111493](https://doi.org/10.1016/j.rse.2019.111493)
- Malmon, D. V., Reneau, S. L., Katzman, D., Lavine, A., & Lyman, J. (2007). Suspended sediment transport in an ephemeral stream following wildfire. *Journal of Geophysical Research*, 112, F02006. doi:10.1029/2005JF000459
- Mansilha, A., Carvalho, P., Guimarães J., Espinha Marques (2014). *Water Quality Concerns Due to Forest Fires: Polycyclic Aromatic Hydrocarbons (PAH) Contamination of Groundwater From Mountain Areas* 806-815
- McCune, B., Mefford, M.J., 2016. PC-ORD. Multivariate Analysis of Ecological Data., MjM Software
- Moody, J. A., & Martin, D. A. (2009). Synthesis of sediment yields after wildland fire in different rainfall regimes in the western United States. *International Journal of Wildland Fire*, 18(1), 96-115
- OECD, 1982. Eutrophication of waters. Monitoring, assessment and control. OECD, Paris, 154 pp.
- Pacheco, F. A., and Fernandes, L. F. S. (2021). Hydrology and stream water quality of fire-prone watersheds. *Current Opinion in Environmental Science & Health*, 21, 100243. doi:10.1016/j.coesh.2021.100243
- R Core Team (2022). R: A language and environment for statistical computing. R Foundation for Statistical Computing, Vienna, Austria. URL <https://www.R-project.org/>
- Robichaud, P. R., Elliot, W. J., Pierson, F. B., Hall, D. E., & Moffet, C. A. (2007). Predicting postfire erosion and mitigation effectiveness with a web-based probabilistic erosion model. *Catena*, 71(2), 229-241
- Rust, A.J., Saxe, S., McCray, J., Rhoades, C.C. and Hogue, T.S., 2019. Evaluating the factors responsible for post-fire water quality response in forests of the western USA. *International Journal of Wildland Fire*, 28(10), pp.769-784.
- Stein, E. D., Brown, J. S., Hogue, T. S., Burke, M. P., & Kinoshita, A. (2012). Stormwater contaminant loading following southern California wildfires. *Environmental Toxicology and Chemistry*, 31(11), 2625-2638.
- Uzun, H., Dahlgren, R.A., Olivares, C., Erdem, C.U., Karanfil, T., Chow, A.T., 2020. Two years of post-wildfire impacts on dissolved organic matter, nitrogen, and precursors of disinfection by-products in California stream waters. *Water Research*, 181, p.115891.
- Vergnoux, A.; Malleret, L.; Asia, L.; Doumenq, P.; Theraulaz, F. (2011) Impact of forest fires on PAH level and distribution in soils. *Environ. Res.*, 111, 193-198
- Wang, M., Jiang, L., Mikelsons, K., & Liu, X. (2021). Satellite-derived global chlorophyll-a anomaly products. *International Journal of Applied Earth Observation and Geoinformation*, 97, 102288
- Wang, Y., Chen, H.-H., Tang, R., He, D., Lee, Z., Xue, H., Wells, M., Boss, E., Chai, F., 2022. Australian fire nourishes ocean phytoplankton bloom, *Science of The Total Environment*, 807, Part 1, 150775, ISSN 0048-9697
- Warren, M.A., Simis, S.G. and Selmes, N. (2021). Complementary water quality observations from high and medium resolution Sentinel sensors by aligning chlorophyll-a and turbidity algorithms. *Remote Sensing of Environment*, 265, p.112651
- Wentworth, G.R.; Aklilua, Y.-A.; Landisb, M.S.; Hsu, Y.-M. (2018). Impacts of a large boreal wildfire on ground level atmospheric concentrations of PAHs, VOCs and ozone. *Atmos. Environ.*, 178, 19-30
- Williamson, C. E., Dodds, W., Kratz, T. K., and Palmer, M. A. (2008). Lakes and streams as sentinels of environmental change in terrestrial and atmospheric processes. *Frontiers in Ecology and the Environment*, 6, 247-254. doi:10.1890/070140
- Williamson, C. E., Saros, J. E., Vincent, W. F., and Smol, J. P. (2009). Lakes and reservoirs as sentinels, integrators, and regulators of climate change. *Limnol. Oceanogr.* 54(6), 2273-2282. doi:10.4319/lo.2009.54.6_part_2.2273

Zhao, Q., Yu, L., Du, Z., Peng, D., Hao, P., Zhang, Y., et al. (2022). An Overview of the Applications of Earth Observation Satellite Data: Impacts and Future Trends. *Remote Sens.* 14, 1863. doi:10.3390/rs14081863

Zheng, Y, Luo X., Zhang W., Wua B., Han F., Lin Z., Wang X. (2012). Enrichment behavior and transport mechanism of soil-bound PAHs during rainfall-runoff events. *Environmental Pollution*, 171, 85-92

9. Annex 1

The .jpg files of the plots of all 154 lakes produced are into the folder “SPR_154lakes”, attached to this Report.

10. Annex 2

The .jpg files of the plots (n=148) of all 74 lakes produced are into the folder “Chl_anomalies_74lakes”, attached to this Report.

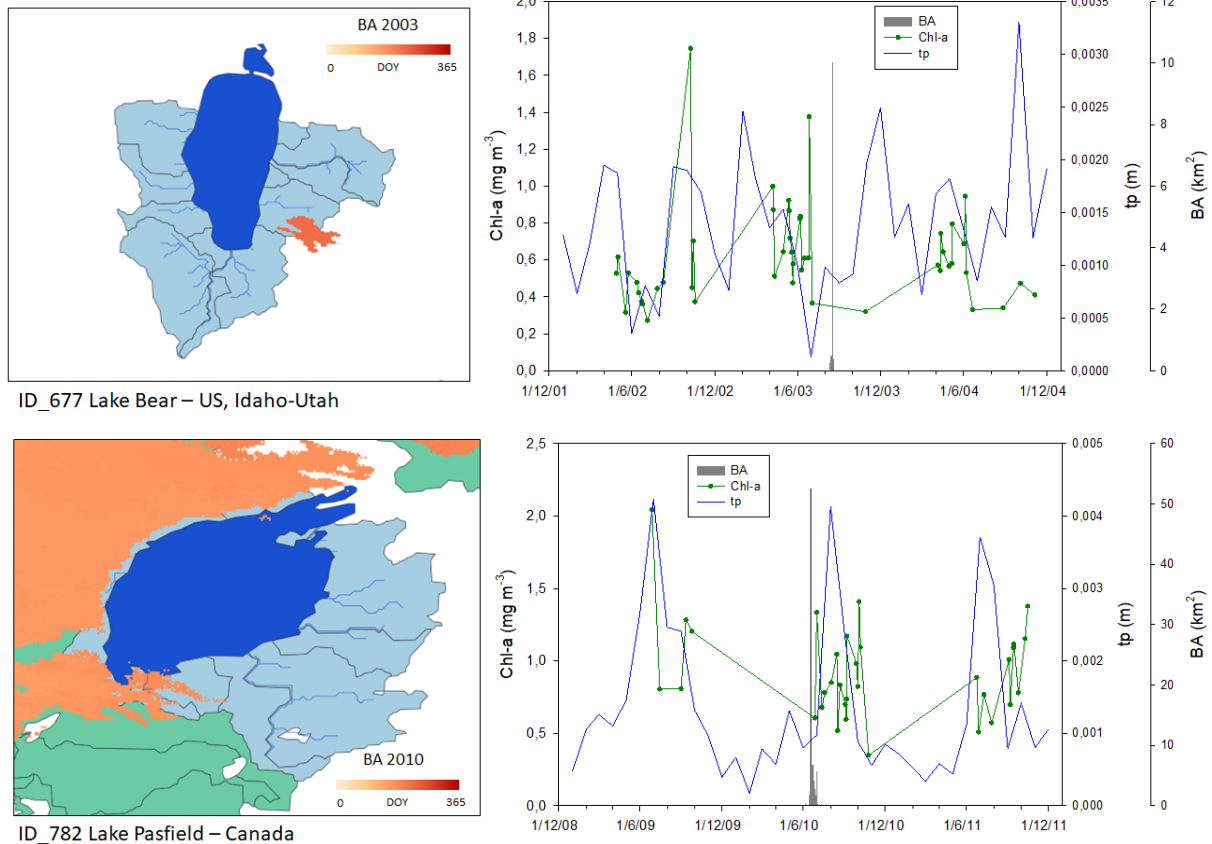


Figure. On the left maps of Bear Lake (ID_677; upper panel) and Pasfield Lake (ID_782; lowe panel) with their catchments, with the distribution and the temporal occurrence of the fires (DOY of burned pixel detection). On the right graphs with Chl-a concentration, total precipitation (tp), and burned area (BA) for the period investigated for each lake.